

Phanerozoic cycles of sea-level change on the Arabian Platform

Bilal U. Haq and Abdul Motaleb Al-Qahtani

ABSTRACT

The Arabian Plate has experienced a complex tectonic history while also being widely influenced by eustatic sea-level changes. These diastrophic events either affected changes in the rate and/or location of subsidence that in turn led to the creation of significant new sedimentary accommodation, or caused major erosional hiatuses. As a result, both eustasy and tectonics have played important roles in the development of sedimentary sequences and in determining the locus and characteristics of reservoir, source and seal facies on the Arabian Platform. Here, we present a synthesis (Cycle Chart) of the regional sea-level fluctuations affecting the Platform that is based on Phanerozoic epi- and peri-Platform sequence-stratigraphic data. Information used for the synthesis includes sections from Saudi Arabia, Kuwait, the Greater Gulf area, Oman and Yemen. The regional Cycle Chart incorporates interpreted sedimentary onlap patterns on the margins of the Arabian Platform, as well as models of regional sea-level fluctuations that controlled these patterns. These are compared to eustatic data that represents the 'global-mean' models of sea-level changes, largely at second-order cycle level for the Paleozoic and third-order cycle level for the Mesozoic and Cenozoic eras. The comparisons reveal that Phanerozoic sediment accumulation patterns on the Platform were broadly controlled by eustasy, with a strong overprint of tectonics for several long intervals. During periods of tectonic quiescence, however, correlations with the eustatic events improve significantly. Thus, for example, during the Cambrian through early Silurian and mid Jurassic through early Paleogene intervals eustasy may have been the significant controlling factor for sedimentary patterns when long-term trends in both regional and global sea-level curves show similarities.

The use of the Cycle Chart could facilitate exploration efforts on the Arabian Platform, provide better chronostratigraphic estimates and global correlations, and prove a useful accompaniment for sequence-stratigraphic studies. This integrative effort was greatly facilitated by the recent publication of the sequence stratigraphic synthesis of the Arabian Plate. The ages of Maximum Flooding Surfaces, however, have been recalibrated to the new (GTS 2004) time scale. This synthesis also represents a new recalibration of the Mesozoic and Cenozoic eustatic curves of Haq et al. (1988) to an up-to-date numerical time scale (GTS 2004).

INTRODUCTION

Over the years, the eustatic cycle chart of sea-level changes for the Mesozoic and Cenozoic based on global synthesis of sequence-stratigraphic data (Haq et al., 1988) has sustained its usefulness as an exploration and first-order global correlation tool. Although geological time scales against which the cycle chart was calibrated have since been refined several times, the overall validity of this synthesis has been corroborated by many independent studies encompassing discrete stratigraphic intervals (e.g., Mitchum and Uliana, 1988; Barron et al., 1991; Bartek et al., 1991; Plint et al., 1992; Miller et al., 1996; Röhl and Ogg, 1996; Pekar and Miller, 1996; Stoll and Schrag, 2000). These studies represent several different approaches to decode base-level fluctuations, ranging from the study of ancient coral reefs and guyots, to continental margins and interior basin stratigraphies, and the use of oxygen isotopes as a proxy for ice volume in the deep-sea record.

The eustatic curves therefore remain valid working models of the long-term trends of the base level, representing marine transgressions and regressions along the world's continental margins, and flooding or desiccation of inland seas and wide interior epi-platform basins. The curves can also be used for first-order correlations worldwide where, or when, tectonic influences are relatively less dominant, i.e. during times of relative tectonic dormancy. In addition, the relative magnitude

and frequency of sea-level rises and falls and the duration of subaerial exposure, as depicted on the eustatic and regional cycle charts, are valuable exploration criteria when considering the response of reservoir and source facies to base-level changes in any given basin.

In siliciclastic and mixed environments, the facility to anticipate the extent of migration of facies as they follow the movement of the base level, or are point-sourced to the basin floor after shelfal incision, can be an important aid in exploration. In carbonate environments, knowledge of the duration of exposure during each cycle as gleaned from the Cycle Chart could provide valuable clues about diagenesis and reservoir quality. Similarly, information about the relative magnitude of sea-level rise and the duration of the highstand during each cycle can also enhance inferences about the production and preservation of organic-rich source rocks. It is not surprising, therefore, that many major exploration companies have adopted the Cycle Chart, and consider it an important component of their exploration toolboxes, often calibrating it to their preferred geological time scales, or adapting it to focus on special target area.

Rationale for an Arabian Platform Cycle Chart

The Arabian Plate has been subjected to an intricate diastrophic history (see e.g., Grabowski and Norton, 1995; Al-Husseini, 2000) in addition to being widely influenced by eustatic sea-level fluctuations (Figure 1). Though the Arabian Shield has remained relatively stable through much of the Phanerozoic, the stratigraphy of the Arabian Platform and peri-Platform basins is a record of major second- and third-order sequences that are separated by extensive regional unconformities. These erosional and/or non-depositional hiatuses were created by major tectonic events on or at the margins of the Platform. One consequence of these tectonic events was to change the rate and/or locus of subsidence that was responsible for the creation or destruction of new accommodation space for sediment accumulation. Thus, both eustasy and tectonics played major roles in the development of sedimentary sequences and in determining the characteristics of the reservoir, source and seal facies on the Arabian Plate.

A regional Phanerozoic Cycle Chart of relative changes of sea level based on the Arabian Platform and peri-Platform basins (Figure 1) that is tied to known eustatic cycles (global "mean") could therefore become a useful exploration tool for the entire Arabian Plate. For example, a direct comparison of the regional events with the global cycles can reveal when tectonic influences were predominant on the Platform, or conversely, when eustasy prevailed in controlling sedimentary patterns. The comparison of the two curves could also yield better chronostratigraphic estimates and improved global correlations in regional studies on and around the Platform. In addition, a regional Cycle Chart would be a useful accompaniment to sequence-stratigraphic studies on the Arabian Platform and surrounding basins in all sedimentary environments.

In predominantly carbonate environments, such as those that prevailed for much of the Mesozoic and Cenozoic on the Arabian Platform, the regional onlap and relative sea-level curves will allow the estimation of the relative magnitude, extent, duration and severity of the sea-level fall events. This, in turn, can permit a better grasp of the broad characteristics of carbonate reservoirs and a better understanding of diagenesis and prediction of porosity and permeability. The regional cycles can also enhance our understanding of the reasons for increased or decreased organic productivity, and thus, source rock production and preservation, as well as the location of effective seals in the stratigraphic column.

In predominantly siliciclastic environments in both marine and non-marine settings, such as those that prevailed for much of the Paleozoic of the Arabian Platform, the use of the regional onlap curve will allow better understanding of the reasons for the extent of lateral migration of reservoir facies, magnitude of incision during sea-level falls and better volumetric estimates of reservoir facies during sea-level falls and organic-rich facies during sea-level rises. Such knowledge could, in turn, lead to better tracking of the location of reservoir facies, such as shoreface, basinal, incised-valley fill, and regressive lowstand and highstand sands. As stratigraphic plays and deeper waters become preferred targets for exploration, such "predictive" capability becomes invaluable.

An additional rationale for the construction of an Arabian Platform-wide Cycle Chart at this time was the publication of Sharland et al. (2001) synthesis of sequence stratigraphy of the Arabian Plate,

which greatly facilitated such an effort. This synthesis has attempted to integrate a vast quantity of Phanerozoic data not only from the Arabian Platform but also from the surrounding basins. Thus, the construction of the Cycle Chart was opportune and was made considerably less time-consuming than it would have been otherwise.

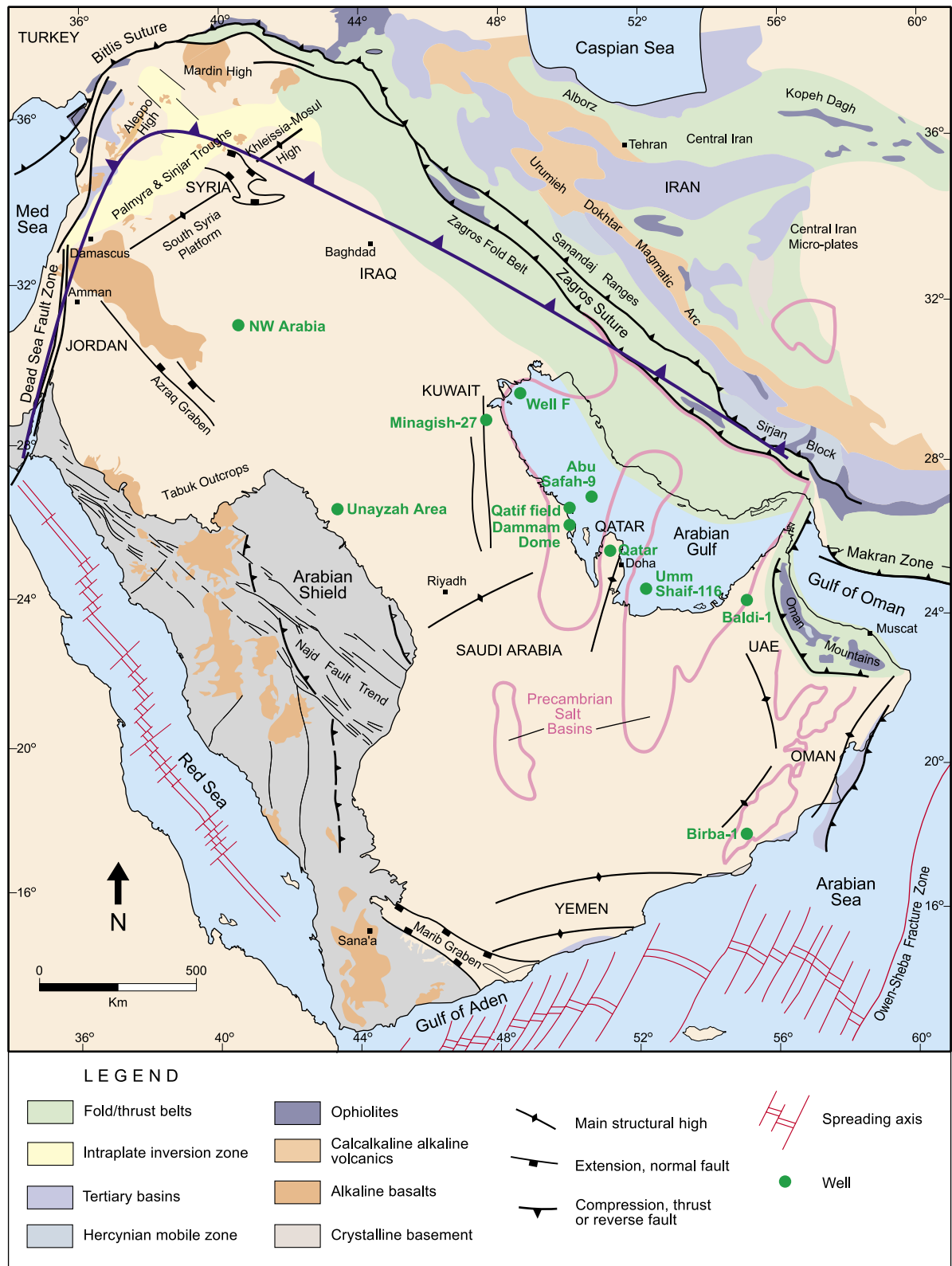


Figure 1: Major tectonic elements of the Arabian Platform and peri-Platform Basins of Yemen, Oman, Arabian Gulf, Southern Iraq, Jordan and the Red Sea (after Konert et al., 2001). Also shown are the locations of the outcrop and well sections included in the Appendix figures that exemplify the process of building regional onlap and sea-level curves.

A BRIEF SYNOPSIS OF TECTONICS OF THE ARABIAN PLATE

The Arabian Plate, a tectonic unit that includes the Arabian Shield, the adjoining Arabian Platform and the surrounding sedimentary basins has been subjected to a complex tectonic history since the Proterozoic (Figure 1). Especially obvious in the stratigraphic record is the evidence of major diastrophic events that caused widespread erosion, peneplanation and/or incision on the Platform. It may be instructive to review the broad Plate-wide tectonic events that governed these patterns so as to discriminate those intervals when the tectonic signal is expected to dominate eustasy. A brief summary of the major events that affected the Plate is given in Table 1.

Through much of the Paleozoic and Mesozoic the Arabian Plate was a part of Gondwana. As evidenced in the Arabian Shield and elsewhere, the Arabian Plate came together as a result of late Precambrian suturing of several terranes of largely basic and dense volcanic and plutonic materials. Once sutured, the composite was prone to long-term subsidence. Variations in the subsequent sedimentary cover reflect the orientation of the mostly northeast and north-northwest trending basement sutures (Al-Husseini, 2000; Ziegler, 2001). The late Precambrian also saw the onset of the northwest-southeast Najd strike-slip movement, which is evidenced from Egypt to Oman, with possible continuation into the then contiguous Indian Plate (Husseini, 1988; Al-Husseini, 2000). This was accompanied by the development of rift basins within which the Hormuz and Ara salt were deposited. Early Cambrian uplift led to widespread erosion and the subsequent Cambrian-Devonian sequences were mostly deposited on a peneplaned platform (Konert et al., 2001). The stratigraphic record on the northeastern shelf indicates gentle subsidence in the Late Cambrian and Early Ordovician, followed by increased subsidence in the mid Ordovician (Sharland et al., 2001) that led to transgressions in this area.

During Late Ordovician times (while the Arabian Plate occupied relatively high southern latitudinal location), a glacial episode occurred which affected the western part of the Arabian Plate, leaving behind evidence of glaciation on the Arabian Shield and broad and deeply cut sub-glacial valleys. The Plate continued to reside in relatively high latitudes until the Early Devonian and persisted as a promontory of Gondwana with passive margins. Thereafter, it started to drift northwards into lower latitudes, reaching tropical environments by Permian times (Konert et al., 2001). In Oman the Late Silurian saw an uplift, which may have been a precursor related to the eventual breakup of Gondwana. This led to a broad regression and stratigraphic gaps on the Platform (Sharland et al., 2001).

The next major deformational event that widely influenced the Arabian Plate was the so-called Hercynian Orogeny. The Hercynian is a term commonly used for Late Devonian to Permian diastrophic movements in Europe and North America. The timing of this orogeny on the Arabian Plate is more restricted (Late Devonian through Late Carboniferous), when the Plate suffered multiple phases of compression and block faulting. The northern edge of the Plate saw initiation of back-arc rifting and basaltic eruption. The compression, uplift of central Arabia and the clockwise rotation of the Plate produced widespread inversion and erosion, leading to the removal of several kilometers of sediment from the uplifted areas (Konert et al., 2001). The Plate then tilted gently towards the northeast and fluvial to alluvial clastics dominated over much of the peneplaned Hercynian relief (Ziegler, 2001).

During the Late Carboniferous and Permian the Arabian Plate moved from the relative high latitudes to lower latitudes, but not before another episode of glaciation near the Carboniferous-Permian boundary that affected the southernmost part of the Plate. The early Permian saw another phase of major crustal extension that weakened the crust enough to allow sediment load alone to drive subsidence and aid in the accumulation of thick carbonate sediments in subtropical latitudes. In the Late Permian further rifting and block faulting along the northeastern front of the Plate, as well in Syria, Iraq and India initiated the splitting of this part of Gondwana. It may also have reactivated the Precambrian Najd Rift system creating north northeast-trending ridges separated by broad valleys (Wender et al., 1998; Sharland et al., 2001). Thus, the Late Permian not only saw the initiation of the continental breakup of this region, but also the creation of a passive margin along most of the northeast boundary of the Plate fronting the newly opened Neo-Tethys Ocean after the Iranian terranes had split and drifted away. This was also the beginning of the dominantly carbonate sedimentation on the Platform over a breakup unconformity. The subsidence at the northeastern passive margin was initially largely post-rift thermal, to be replaced by dominantly due to sediment loading (Bishop, 1995).

TABLE 1
Major Phanerozoic tectonic events that influenced sedimentary patterns on the Arabian Platform
(after Grabowski and Norton, 1995, and Sharland et al., 2001)

System/Series	Tectonic Event	Subsequent Arabian Plate Effects
Late Precambrian	Najd shear-zone-related rifting begins	Development of rift salt basins to be filled with continental clastics
Early Cambrian	Subsidence starts after peneplanation	Transgressions of the Platform in Late Cambrian and Early Ordovician
Latest Ordovician	Hinterland is uplifted	Major hiatus and down-cutting on Platform
Latest Devonian	'Hercynian' Orogeny begins on Arabian Plate	Multiple phases of compression and block faulting. Widespread inversion, erosion of several km of sediments on the Platform
Latest Carboniferous	End of 'Hercynian' Orogeny on Arabian Plate	Plate tilts gently to the northeast
Late Permian	Neo-Tethys opens and the NE passive margin begins to subside	Transgression and beginning of dominantly carbonate sedimentation over the Platform
Early Jurassic	Rifting of India from Africa/Arabia begins	India separates from Gondwana by Late Jurassic. Plate tilts toward north.
Late Early Jurassic	Rifting starts in eastern Mediterranean and western margin of Plate	Uplift of western margin of the Plate, beginning of a passive margin along northwestern margin of the Plate
Early Cretaceous	South Atlantic begins to open	Plate tilts more to the east and dominant sediment transport is now from west to east.
Mid Cretaceous	Mediterranean begins to open	Sub-basins form on Arabian Platform
Late Cretaceous	Ophiolite obduction along NE margin begins	Fault reactivation and uplift of NE margin of Platform
Early Paleocene	Ophiolite obduction ends	Erosion along NE margin of Platform
Late Eocene	Closure of Tethys Seaway	Arabian Plate begins its collision with Asia and tilts again to the northeast
Late Oligocene	Gulf of Aden and Red Sea starts to open	Eastern branch of Tethys closed by this time

The next major tectonic event was initiated in the Early Jurassic when the Indian Plate first began to split from Gondwana (Grabowski and Norton, 1995), completing its separation from Arabia in the Late Jurassic. Rifting in the central Mediterranean also began in the Early Jurassic, affecting the northern part of the Arabian Plate. Late Early Jurassic rifting at the northwestern boundary of the Plate led to later development of a new passive margin and new accommodation space along this subsiding shelf (Sharland et al., 2001).

The Mediterranean rifting continued into the Early Cretaceous, which may have been partially responsible for uplifting in western Arabia (Grabowski and Norton, 1995). Also by the Early Cretaceous, separation of India from Arabia had been accomplished and a new ocean had begun to open between the two Plates. The southern Oman margin was now also a subsiding passive margin, open to transgression. The far-field opening of the central and south Atlantic at this time may have also contributed to the uplift of the western part of the Arabian Plate and changed the gentle northeastward tilt of the Plate to the east. This shifted the dominant sediment transport direction, i.e. eastward from the uplifted area that supplied large volumes of sediments to the Platform (Al-Fares et al., 1998; Sharland et al., 2001). In the mid Cretaceous a new short-lived spreading ridge system formed off the northeastern margin of the Arabian Plate, most likely related to changes in the motion

of the Indian Plate. In the early Late Cretaceous, accelerating convergence between the Arabian and Asian Plates led to the obduction of this new Neo-Tethyan oceanic crust as ophiolites along the northeastern margin of the Arabian Plate. This convergence also exerted compressive stresses over the Plate and caused uplift and erosion over many of the re-activated arches and anticlines.

The Cenozoic tectonic history of the Arabian Plate is largely that of continued rapid convergence between the Plate and Eurasia and the closure of the eastern part of the Neo-Tethys seaway. Much of this convergence was accommodated by subduction along the northern margins of the shrinking Tethys seaway, under the Iranian terranes and the Makran subduction zone of Pakistan. In the late Eocene the Plate began to collide with Asia and the closure of the Neo-Tethys was essentially complete by the late Oligocene. The Plate once again was tilted to the northeast due to rifting along the western margin and structural loading in the northeast. Rifting in the Gulf of Aden and Red Sea may have been initiated in the late Oligocene (Hughes et al., 1991), but it manifested itself fully in the mid to late Miocene, most likely aided by loading of the eastern part and flexing of the Plate (Sharland et al., 2001).

It is apparent from the above summary that the Arabian Plate suffered several long-term periods of tectonic deformation that alternated with periods of relative quiescence. The largely cyclic record of sedimentary patterns will reflect the influence of tectonism by displaying major gaps and less concurrence with the eustatic curves, which represent a mean global model, during the periods of upheaval, while intervals of relative stability will show greater correlation with eustasy.

CONSTRUCTION OF THE CYCLE CHART FOR THE ARABIAN PLATFORM

The Arabian Platform Cycle Chart was initially constructed based on existing plate-wide data from the public domain. It was later revised and refined and with the assistance of explorationists from Saudi Aramco, who offered invaluable information based on their experiences from the sedimentary sections they were familiar with. Following is a brief description of the various sections of the Cycle Chart and the data upon which they are based.

Geological Time Scales

A careful selection of Paleozoic and younger time scales for the calibration of cycles of sedimentation and attendant tectonic events is a crucially important first step in the construction of a cycle chart. The inherent problems with building time scales and the array of sources of error in various dating criteria (e.g., radiometry, biostratigraphy, magneto-stratigraphy, isotopic-stratigraphy) have been discussed in some detail in Haq et al. (1988) and will not be repeated here. However, these authors suggested that a meaningful time scale must make no unnecessary assumptions about constancy of rates of various events used to calibrate time scales (e.g., biological evolution, sea-floor spreading, etc.). It must also incorporate a large body of good radiometric dates to discern significant trends in the data, rather than relying on a few chosen dates as "tie points" to pin down segments of the time scale. And above all, it must use multiple, overlapping correlative criteria to reduce the noise to signal ratio (see Haq et al., 1988, for details). Though we still have a long way to go in producing a truly acceptable time scale that overcomes all of these caveats, especially for the older Periods, it should be noted that in recent years the new time scales are converging towards this philosophy. Thus, while good bio- and chrono-stratigraphic resolution is now available for the younger Periods (i.e. the Late Cretaceous through Cenozoic interval) that allows meaningful wider correlations, the older part of the stratigraphic column still suffers from lack of such resolution and true wider correlatability.

This is exemplified by parts of the Paleozoic time scale, especially the Precambrian/Cambrian boundary and the earlier Paleozoic, which has been in a state of considerable flux over the last two decades. New numerical dates have shown the Cambrian/Precambrian boundary to be some 48 million years (my) younger than previous estimates (i.e. 542 Ma vs 590 Ma). Many of the younger boundaries of the Paleozoic have also been modified significantly (e.g., Ordovician/Cambrian, Devonian/Silurian, Carboniferous/Devonian and Permian/Carboniferous boundaries have all been modified by several million years). Similarly, there have also been refinements of up to several my in the placement of the Mesozoic Epoch (and sub-epoch) boundaries (especially in the Triassic), and, to a lesser extent, in the Cenozoic.

After considering the nuances of all the available geological time scales, we had originally adopted the time scale summarized by Gradstein and Ogg (1996) for the construction of the Arabian Platform Cycle Chart. These authors had presented a composite time scale of the three Eras of the Phanerozoic based on three different time scales. They essentially used the Harland et al. (1990) time scale for the Paleozoic, the Gradstein et al. (1994) time scale for the Mesozoic, and Berggren et al. (1995) time scale for the Cenozoic. One of the added advantages of using this composite was that it was in wide use and had also been adopted by Sharland et al. (2001) for their synthesis of the Arabian Plate stratigraphy and its use would have facilitated direct comparisons, especially in assignment of ages of the major maximum flooding surfaces (MFSs) identified by these authors. However, since the submission of this paper for publication a new composite time scale (Gradstein et al., 2004) known as the Geological Time Scale 2004 (GTS 2004) was presented at the International Geological Congress in Florence, Italy, that has the concurrence of the International Commission on Stratigraphy. Much of the Paleozoic and Mesozoic (with the exception of Late Cretaceous) has been modified in the GTS 2004 over the old (Gradstein and Ogg, 1996) version. We have adopted GTS 2004 and have revised the Arabian Platform Cycle Chart accordingly. This entailed recalibration of the major MFSs of Sharland et al. (2001, 2004) to the new numerical time scale. This recalibration is presented in Table 2. As an added consequence, the Haq et al. (1988) eustatic curves have also been recalibrated to GTS 2004 for the first time, and presented on the accompanying Cycle Chart.

Arabian Platform stratigraphy and chronostratigraphy

Since a Cycle Chart with an abundance of stratigraphic names from the Platform, often different in different countries for the same formation, would have been too cumbersome, the formation and member names have been largely adopted from the existing stratigraphic nomenclature from Eastern Saudi Arabia. Regional equivalents of these names in other countries are well established, and can be found in a number of key country-specific papers, as well as platform-wide comparisons (e.g. Powers, 1968; Sugden and Standring, 1975; Hughes Clark, 1988; Hassan, 1989; Chaube and Al-Samahiji, 1995; Yousif and Nouman, 1997; Al-Husseini, 1997; Christian, 1997; Sharland et al., 2001, and the references therein). As an initial step the chronostratigraphic extent of the formation and members was plotted following Sharland et al.'s (2001) synthesis of the ages of the Formation boundaries. These boundary placements were further refined following discussions with specialists from Saudi Aramco based on existing data. Thus, the stratigraphic extent of the formations/members shown is a "consensus" and does not necessarily conform to any individual opinion. Similarly, the general i.e. gross lithology of the formations also follows Sharland et al. synthesis, but was modified after discussions with specialists. For simplicity, the lithological units are distinguished only into four major types: sandstone, shale, carbonate and evaporite.

Regional onlap and sea-level curves

On the Arabian Plate much of the ocean's transgressive activity that inundated the Platform was from the present north and the northeastern directions, while sediment supply was mostly from the western highs toward the north and northeast. Thus, the dominant sediment onlap patterns also trend from the north and northeast and as is to be expected, sections are in general more completely preserved basinward i.e. toward the northeast.

The procedure for constructing an onlap curve for the Arabian Platform comprises a region-wide approach. As far as possible, sections from Saudi Arabia were used to determine the position of the maximum flooding surfaces (MFS) and the intervening sequence boundaries (SB). However, when no sections from Saudi Arabia were available, either due to non-deposition/erosion in those intervals or because none have as yet been studied, sections from neighboring Oman, Yemen, southern Iraq and the Greater Gulf were used to fill the gaps. This is especially true for periods when the sea level withdrew below Platform top or tectonics led to extensive erosion on the Platform. During such times sea-level history is preserved only on the margins of the Platform or in the incised valleys, making it necessary and appropriate to include the peri-Platform sections in a regional sea level synthesis. Consequently, it should be underscored that the resultant onlap curve is for the whole region of the Arabian Platform and its margins and not limited to Saudi Arabia. It should be noted, however, that sections from deformed margins of Turkey and Iran were not included. These areas have undergone dramatic tectonic events, implying that local tectonics may sufficiently complicate the record that it may be at variance with that of the Platform.

The flooding of the Platform surface is represented first by deposition of the transgressive deposits (transgressive systems tract – TST) overlain by deposits of the highstand systems tract (HST). Lowstand (lowstand systems tracts – LST) equivalents are only preserved on the Platform within incised valleys (as incised valley fills). Although Sharland et al. (2001) did not identify sequence boundaries, they attempted to date major maximum flooding surfaces (MFSs) and tie them regionally. Consequently, it was considered practical and advantageous to use the major regional MFSs identified in this synthesis as a starting point for constructing the onlap curve (recalibrated to GTS 2004 for the numerical time scale, see Table 2). However, these authors underscored that the identification and age assignment of many MFS, especially those in the Paleozoic and Triassic, are fraught with numerous uncertainties. These include both the uncertainties of actual physical placement of MFSs within a section and biostratigraphic dating, as well as uncertainties in their calibration to the absolute time scales (see Sharland et al., 2001, p. 52). Thus, sequence boundary ages as identified here suffer even more from the uncertainties ascribed to the dating of MFSs, the latter being normally much better constrained than the hiatuses represented by sequence boundaries.

At present no meaningful approach exists to determine the absolute scale (in meters) of rises and falls of sea level. All of the various methodologies (e.g. coastal aggradation during highstands, extent of marine inundation, depth of shelf incision during lowstands, changes in fossil paleobathymetry, oxygen-isotopic variations reflecting ice-volume fluctuations, etc.) have inherent uncertainties and imply considerable error ranges. Thus, instead of trying to estimate the absolute movement of base level in meters (with significant error bars), a relative scale has been used for the construction of the onlap curve and the sea-level curve that is based on it.

In a series of paleofacies reconstructions of the Arabian Plate for the Permian to Holocene interval, Ziegler (2001) has produced a valuable graphic history of marine inundation (and relative water depth) and subaerial exposure of the Platform. These paleofacies maps have been very helpful in assigning the relative magnitude of the sea-level fluctuations, as was the discussion of the overall paleofacies in Sharland et al. (2001). The approximate position of the Platform surface, i.e. not the entire surface, but its lowest mean elevation, has been identified as a useful marker level for the onlap curves. In this regard it should be noted that even though much of the central Platform may be bare during some intervals, shallow-marine, or even deeper marine facies may continue to be deposited in some peri-Platform basins, e.g. the Middle Cambrian paleofacies map in Konert et al. (2001). In such cases, local relative base-level height would need to be adjusted when consulting the Cycle Chart. Clues to the long-term behavior of sea level are provided by several indicators: (1) the flooding of the Platform surface, indicated by preservation of extensive marine deposits; (2) the thickness of the sections preserved on or off the Platform; (3) the depth of incision and the nature and thickness of sediments preserved in incised valleys and on distal shelf and slope; and (4) paleobathymetric estimates from litho- and biofacies. These data provide the template against which the shorter-term relative sea-level changes can be scaled, i.e. mostly third-order cycles, but occasionally fourth-order cycles as well, when these can be recognized consistently over a wide area.

Once the overall regional onlap patterns were in place, individual sections were consulted to interpret the details. Sequence boundaries and additional maximum flooding surfaces, as well as transgressive surfaces (TSs) and lowstand equivalents, where they could be identified, were demarcated from these sections. The individual sections considered (see some of the examples in the Appendix) are mostly those from the Sharland et al. (2001) synthesis, which has the advantage that they are all in the public domain, have all been treated in a uniform manner, and that attempts to date individual horizons according to internally consistent criteria.

The relative sea-level curve for the Arabian Platform is a derivative of the regional onlap curve. While the onlap curve shows a saw-toothed pattern, because of the continued coastal onlap above the maximum flooding surfaces, represented by the deposition of non-marine fluvial and near-coastal sediments during the regressive part of the highstand, the relative sea-level change curve shows individual events as more sinusoidal (as the sea began to recede after the maximum flooding surface was reached). Another difference is that the onlap curve is scaled against an approximate marker level of the Platform top, while the relative sea-level curve is scored against the modern base level for convenience. Thus, the onlap curve can be thought of as representing the changes in the sedimentary patterns, while the relative sea-level curve represents the actual changes in the base level that drove the stratigraphic changes.

TABLE 2
Ages of the numbered major Arabian Plate Maximum Flooding Surfaces (Sharland et al., 2001, 2004) as recalibrated to GTS 2004 (Gradstein et al., 2004) and used on the Cycle Chart.

Major Maximum Flooding Surface (Sharland et al., 2004)	Stratigraphic Position (Sharland et al., 2001, 2004)	Age (in Sharland et al., 2001, 2004)	Recalibrated Age (recalibrated to GTS, 2004)
Ng40	Miocene (Langhian)	15.5 Ma	14.6 Ma
Ng30	Miocene (Langhian)	16.3 Ma	15.9 Ma
Ng20	Miocene (Burdigalian)	18.5 Ma	18.5 Ma
Ng10	Miocene (Burdigalian)	20 Ma	20 Ma
Pg50	Oligocene (Chattian)	24.5 Ma	24 Ma
Pg40	Oligocene (Rupelian)	29 Ma	29 Ma
Pg30	Oligocene (Rupelian)	33 Ma	33 Ma
Pg20	Eocene (Lutetian)	49 Ma	48.6 Ma
Pg10	Paleocene (Selandian)	58 Ma	59 Ma
K180	Late Cretaceous (Maastrichtian)	68 Ma	68 Ma
K170	Late Cretaceous (Campanian)	78 Ma	78 Ma
K160	Late Cretaceous (Santonian)	85 Ma	85 Ma
K150	Late Cretaceous (Coniacian)	88 Ma	88 Ma
K140	Late Cretaceous (Turonian)	93 Ma	93 Ma
K130	Late Cretaceous (Cenomanian)	95 Ma	95 Ma
K120	Late Cretaceous (Cenomanian)	98 Ma	98 Ma
K110	Late Cretaceous (Albian)	101 Ma	101 Ma
K100	Late Cretaceous (Albian)	106 Ma	106 Ma
K90	Late Cretaceous (Albian)	111 Ma	111 Ma
K80	Early Cretaceous (Aptian)	116 Ma	117 Ma
K70	Early Cretaceous (Aptian)	120 Ma	122.5 Ma
K60	Early Cretaceous (Barremian)	123 Ma	126 Ma
K50	Early Cretaceous (Barremian)	126 Ma	129 Ma
K40	Early Cretaceous (Hauterivian)	129 Ma	132 Ma
K30	Early Cretaceous (Valanginian)	136 Ma	139 Ma
K20	Early Cretaceous (Berriasian)	138 Ma	141 Ma
K10	Early Cretaceous (Berriasian)	143 Ma	144 Ma
J110	Late Jurassic (Tithonian)	147 Ma	147 Ma
J100	Late Jurassic (Tithonian)	150.75 Ma	150.75 Ma
J90	Late Jurassic (Kimmeridgian)	151.25 Ma	151.5 Ma
J80	Late Jurassic (Kimmeridgian)	151.75 Ma	152.5 Ma
J70	Late Jurassic (Kimmeridgian)	152.25 Ma	154 Ma
J60	Late Jurassic (Kimmeridgian)	154 Ma	155 Ma
J50	Late Jurassic (Oxfordian)	156 Ma	158 Ma
J40	Middle Jurassic (Callovian)	162 Ma	163 Ma
J30	Middle Jurassic (Bathonian)	168 Ma	167 Ma
J20	Middle Jurassic (Bajocian)	175 Ma	170 Ma
J10	Early Jurassic (Toarcian)	185 Ma	180 Ma
Tr80	Late Triassic (Norian)	215 Ma	211 Ma
Tr70	Late Triassic (Carnian)	222 Ma	220 Ma
Tr60	Late Triassic (Carnian)	226 Ma	226 Ma
Tr50	Middle Triassic (Ladinian)	233 Ma	234 Ma
Tr40	Middle Triassic (Anisian)	238 Ma	241 Ma
Tr30	Early Triassic (Induan)	245 Ma	249.75 Ma
Tr20	Early Triassic (Induan)	246 Ma	250 Ma
Tr10	Early Triassic (Induan)	247 Ma	250.5 Ma
P40	Late Permian (Wuchiapingian)	249 Ma	254 Ma
P30	Late Permian (Wuchiapingian)	250 Ma	255 Ma
P20	Middle Permian (Capitanian)	252 Ma	261 Ma
P10	Early Permian (Sakmarian)	272 Ma	287 Ma
C10	Middle Mississippian (Visean)	333 Ma	333 Ma
D30	Late Devonian (Famennian)	355 Ma	361 Ma
D20	Early Devonian (Emsian)	393 Ma	401 Ma
D10	Early Devonian (Pragian)	402 Ma	408 Ma
S20	Late Silurian (Ludlovian)	418 Ma	418 Ma
S10	Early Silurian (Aeronian)	440 Ma	440 Ma
O40	Late Ordovician (Caradoc)	453 Ma	454 Ma
O30	Middle Ordovician (Llanvirn)	465 Ma	469 Ma
O20	Early Ordovician (Tremadoc)	487 Ma	483 Ma
O10	Early Ordovician (Tremadoc)	494 Ma	486 Ma
Cm30	Late Cambrian (Merioneth)	502 Ma	496 Ma
Cm20	Middle Cambrian (St. David)	510 Ma	506 Ma
Cm10	Early Cambrian (Nemakit-Dal)	540 Ma	538 Ma

Reservoir, known and potential source-rich intervals

Known reservoir intervals and their nomenclature (as shown on the Cycle Chart) are largely those from Eastern Saudi Arabia, and have been differentiated into oil, non-associated gas, and oil plus gas reservoirs. In addition to the known reservoirs, lowstand incised valley fills may also prove to be good local reservoirs with considerable extent. The known source rock intervals are adopted from Sharland et al. (2001), whilst potential source rock intervals include 'condensed' sections associated with maximum flooding surfaces identified by Sharland et al. as well as other intervals interpreted here.

Systems tracts

The column between the regional onlap and relative sea-level curve contains the interpretation of the systems tracts associated with each identifiable sequence. In most cases, lowstand systems tracts (LST) cannot be separated from transgressive systems tracts (TST) and these are lumped together below the MFS. On the Platform itself the lowstand interval would span the time of the erosion associated with the sea-level fall, represented by the SB, overlain directly by transgressive deposits, thus, on the Platform top, the LST does not occur physically but only in the sense of an equivalent time gap. However, this interval may include a lowstand component on the Platform margins, as for example incised valley fill, or in the basin as a lowstand wedge and/or fan. The generally upward-deepening TST sediment packages are overlain by the commonly upward-shoaling deposits of the highstand systems tracts (HST). The sequence numbering (or rather the MFS numbering, e.g. P10, P20, P30, Tr10, Tr20, Tr30, etc.) follows the Sharland et al. (2001, 2004) scheme.

Stratigraphic sections used for detailed interpretations

Information on the Cambrian sequences (Upper Hormuz Salt, Siq, Burj and lower part of Saq formations) comes mostly from Oman. These sections include the upper part of the Huqf Supergroup, the Ara Group, the Haima Supergroup and Ghaba Salt Basin, southeastern Oman (after Gorin et al., 1982; Hughes Clark, 1988; Droste, 1997; and modifications in Sharland et al., 2001). (See also the Appendix for examples).

For the Ordovician and Silurian sequences (the upper part of Saq, Qasim, Sarah, Qalibah and lowermost Tawil formations in Saudi Arabia and their chronostratigraphic equivalents elsewhere) several sections are exposed in central Saudi Arabia (after Vaslet, 1990; Mahmoud et al., 1992; Senalp and Al-Duaiji, 2001b). For Devonian sequences (upper Tawil, Jauf and much of Jubah formations and their equivalents) sections are encountered in the Ghawar area and in northwestern Saudi Arabia (after Wender et al., 1998; Boucot et al., 1985; and modifications in Sharland et al., 2001). The Carboniferous (upper part of Jubah and the Berwath formations and their equivalents) stratigraphic information largely comes from the Greater Gulf area (Clayton et al., 2000). For the Permian (Unayzah and Lower Khuff formations and their equivalents) information is drawn from central Saudi Arabia (McGillivray and Hussein, 1992; Senalp and Al-Duaiji, 1995 and 2001a; Evans et al., 1997; and Al-Aswad, 1997), the Ghawar area (Wender et al., 1998) and the Greater Gulf area (El-Bishlawy, 1985) (See also the Appendix for examples).

Details of the Triassic sequences (Upper Khuff, Sudair, Jilh and Minjur formations and their equivalents) were gleaned from sections in the Greater Gulf area and Oman (after Loutfi and Sattar, 1987; Hughes Clarke, 1988) (see Appendix). Note that the Minjur Formation is placed completely within the Late Triassic. The Jurassic sequences (Marrat, Dhurma, Tuwaiq Mountain, Hanifa, Jubaila, Arab, Hith and Sulaiy formations and their equivalents) have been identified in sections from central Saudi Arabia, Oman, Yemen, Kuwait and the Greater Gulf area (after Enay et al., 1987; Hughes Clarke, 1988; Droste, 1990; Yousif and Nouman, 1997; Howarth and Morris, 1998; Azer and Peebles, 1998; and modifications in Sharland et al., 2001). Information about the Lower Cretaceous (Yamama, Buwaib, Biyadh and Shu'aiba formations and their equivalents) and the Upper Cretaceous sequences (Wasia and Aruma formations and their equivalents) is drawn from outcrop sections in Oman and largely subsurface data from Yemen, Kuwait and the Greater Gulf area (after Hughes Clark, 1988; Simmons, 1990; Holden and Kerr, 1997; Brannan et al., 1997; Hughes, 2000; Philip et al., 1995; Brennan, 1990;

Al-Fares et al., 1998; Aziz and Sattar, 1997; Alsharhan, 1987; Pascoe et al., 1995; Smith et al., 1995; and modifications in Sharland et al., 2001).

The Paleogene sequences (Umm er Raduma, Rus and Dammam formations and their equivalents) are based on sections in eastern Saudi Arabia, Yemen and Oman (Hasson, 1985; Hughes Clark, 1988; Nolan et al., 1990; Brannan et al., 1997; Weijermars, 1999). The Neogene information (for Hadruk, Dam, Hofuf and Dibdibba formations and their equivalents) comes largely from Oman (Hughes Clark, 1998).

Global onlap and sea-level curves

The global onlap and its derivative sea-level curves are plotted next to regional curves for comparison. For the Paleozoic the onlap curve is largely a curve of second-order events. It is a composite that uses the long-term trends of Vail et al. (1977) and Hallam (1992) Paleozoic curves (calibrated to the new GTS 2004 time scale used here) as a template and builds on it for details with additional information from other areas. To exclude purely local events, only those events are depicted on the global 'mean' curve that are common to several different basins. Additional information is based on: (1) the published curves of Ross and Ross (1988), a synthesis that includes widely distributed data (though mostly from the United States interior basins); (2) the Devonian synthesis of Euramerica (Johnson et al., 1985); (3) Ordovician to Devonian of western and northern Canadian basins (Lenz, 1982); (4) late Paleozoic of northwestern China (Chen and Shi, 2003), and published information from North Africa (Keeley, 1989; Schandelmeier and Reynolds, 1997); recent work on the Algerian Paleozoic by Yahi et al., 2001); as well as (5) unpublished data from US interior basins. It must be underscored that the Paleozoic global curve is chronostratigraphically much less well constrained than those for younger Eras and should be considered approximate at best. Nevertheless, it represents an adequate working model, especially for the long-term trend of the base-level fluctuations, i.e. at the level of second-order cycles, and for some intervals at third-order level. As better-constrained chronostratigraphic data accumulates, refinements of the Paleozoic curves are to be expected, especially in identifying more third-order events.

The Mesozoic and Cenozoic part of the global curve (with identified third-order cyclic eustatic events) is based on Haq et al. (1988), rescaled and tied to the time scale adopted here. This global "mean" working model also includes only those sea-level change events that were documented in several widely distributed basins to establish that these fluctuations were of broad extent. The cycles were also tied directly to the standard European chronostratigraphy (i.e. stage stratotypes) to facilitate worldwide correlations. The recalibration of eustatic curves to GTS 2004 (presented on the accompanying Cycle Chart) in itself provides an expedient update of this widely used working model for exploration and paleoceanographic studies.

Major tectonic, paleoceanographic and climatic events

The major tectonic events column comprises both the regional (Arabian Plate) and the global events. These are based on various sources, including Grabowski and Norton (1995), Haq and van Eysinga (1998), Konert et al. (2001), and Sharland et al. (2001), among others.

The paleoceanographic and climatic events' column also includes those events that occurred specifically on or around the Arabian Platform, as well as global events. These are largely based on Sharland et al. (2001) for local glaciations, and Haq and van Eysinga (1998) for all other global events. The experience and views of Saudi Aramco specialists were also taken into account in completing these columns.

Tectonostratigraphic megasequences

For comparison, in the right-hand column, the chart also includes the extent of the tectonostratigraphic megasequences as defined by the Sharland et al. (2001) synthesis (their boundaries have been recalibrated to GTS 2004). These authors have identified eleven Arabian Plate megasequences (AP1-AP11) that are separated by major unconformities caused by tectonic events.

DISCUSSION

The preceding sections outlined the procedure followed for integrating regional cycles of sediment deposition and erosion, driven by base-level changes, on and around the Arabian Platform. The regional cycles are plotted against the 'global' model of sedimentary cyclicity. In this regard it needs to be underscored that the few, if any, 'global' events are ever worldwide or their effect ever instantaneous, and the magnitude of change at various places may differ depending on local conditions. Eustasy is no exception. Hence, the global curve can only be seen as an "average" (or a most likely scenario) during times of relative tectonic quiescence. If a comparison of the regional patterns with the global patterns reveals that during a discrete time interval the trends in regional cyclicity mimics global cyclicity, it indicates that eustasy was the dominant control on sedimentary patterns. Other intervals that show little or no correspondence between regional and global patterns imply an overriding control by tectonic and other factors.

Even a cursory look at the Cycle Chart reveals that there were several conspicuous and long periods of hiatus in sedimentation on the Arabian Platform. The older of such enduring (c. 25 my in duration) period of hiatus lasted through much of the Carboniferous and was linked to multiple phases of compression and deformation and/or inversion during the Hercynian Orogeny that led to the erosion of several kilometers of sediments on the Platform. The next younger major period of hiatus (c. 20 my in duration) lasted from latest Triassic through the Early Jurassic and was associated with a phase of the breakup of Gondwana that led to the rifting of India from Arabia/Africa and tilting of the Arabian Plate towards the north. The youngest major period of hiatus (c. 10 my in duration) occurred in the Oligocene, which may have been a consequence of the collision of the Arabian Plate with Eurasia and the closure of the eastern limb of Neo-Tethys Ocean. There was also a major draw-down of sea level starting in latest Eocene due to initiation of major buildup of ice cap on Antarctica.

A comparison of the regional and the global cycles reveals that while the Platform was gently subsiding during the Cambrian through early Silurian interval, eustasy may have been an important if not the principal controlling factor that determined sedimentary patterns. The two curves (on the Cycle Chart) show similar long-term trends, though there are more relative sea-level change events identified on the Platform. This is not surprising since the global curve shows mostly second-order cycles for much of the Paleozoic, while many of the Arabian Platform sequences may represent third-order or even higher-order cycles. There is a sharp sea-level drop in the Late Ordovician, on both the Arabian Platform and the global curves, which may be attributable to the glacial episode that affected this part of Gondwana at that time.

From late Silurian through Early Carboniferous the regional and global curves show little correspondence. The long-term trend on the Arabian Platform is of a continued regional sea-level rise, while on the global curve much of Devonian through Carboniferous interval saw a gradual sea-level fall. These differences can be ascribed to active tectonics that obscure the underlying eustatic signal. Uplift in Oman in the mid Silurian, which was a precursor to continental breakup, and the beginning of Hercynian compression and the erosional episodes that followed in Late Devonian may have been partially responsible for these differences. Widespread inversion and erosion during the Hercynian Orogeny was responsible for removal of much of the late Carboniferous sediments making it difficult to reconstruct the history of sedimentary cyclicity for this interval on the Platform. The early Permian regional cycles most likely were also influenced by tectonics when the Platform suffered through another phase of major crustal extension with the rifting of the Neo-Tethys margin. However, glacial episodes in the late Carboniferous and early Permian on the Arabian Platform and the Southern Hemisphere (with global repercussions) make the fluvio-glacial record of this interval (preserved as valley fills) of the Platform and elsewhere (e.g. northwestern China – see Chen and Shi, 2003) look similar. Mid Permian sea-level drop is more prominent on the global curve than it is on the Arabian Platform and the late Permian through Triassic record is well developed on the Platform when the Arabian Plate gradually moved into the equatorial latitudes.

The record of latest Triassic through Early Jurassic (Rhaetian through Pliensbachian) is also largely missing from the Platform due to erosion or non-deposition. This break may be related to major tectonic events that initiated the splitting of the Indian Plate from Gondwana and Arabia and rifting in the central Mediterranean in the Early Jurassic. These events affected a good deal of eastern and northern parts of the Arabian Plate. Through much of the remainder of the Mesozoic and early Paleogene sedimentary cycles on the Platform show good agreement with the eustatic patterns, both

in the longer-term trends and the frequency of third-order events, though the number of events in some discrete intervals differ. The only exceptions to this general correspondence are in the latest Jurassic through Early Cretaceous (mid Tithonian to mid Valanginian) interval, although the long-term trends are similar. These differences, once again, may be due to the continued rifting in the Mediterranean that lasted into Early Cretaceous, and the beginning of the opening of the Atlantic Ocean, both of which may have led to the uplift of western Arabia. Also, the Turonian sea-level drop seems to occur slightly earlier on the Platform than on the global curve, but this may be an artifact of the placement of the upper limit of the major unconformity within this stage. These overall trends indicate that from Middle Jurassic through the early Eocene eustasy was the dominant control over sedimentary sequences on the Platform. In their study of the Jurassic and Cretaceous stratigraphy of the central Arabian Platform, Le Nindre et al. (1990) also reached the conclusion that in these periods eustatic changes appear to be responsible for sedimentary patterns on the Platform.

The late Paleogene of the Platform and Neogene of the peri-Platform basins (Oman) show longer-term trends similar to the global curve, though the rich number of third-order events seen on the global curve are much less numerous regionally. This is to be anticipated since the tectonic influence was dominant after late Eocene times, as the Tethys Seaway began to close, and especially after the early Miocene as the Zagros Mountains began to emerge along the northeastern margin of the Plate, causing the sea to retreat from much of the Platform.

ACKNOWLEDGEMENTS

The Arabian Platform Cycle Chart was first published at the American Association of Petroleum Geologists' meeting in Cairo, Egypt in October 2002 (Haq and Al-Qahtani, 2002 and Al-Qahtani et al., 2002). The authors thank Saudi Aramco for the opportunity to construct the Cycle Chart and for the approval for its publication. The Chart was refined with the help of specialists in Saudi Aramco's various mapping groups: Bassam Bahabri, Roger Price, Kent Norton, Muhittin Senalp, Christian Heine, Geraint Hughes, Sa'id Al-Hajiri, Abdelghayoum Ahmad, Abdel Fattah Bakhiet and Mike Hulver. Their help is gratefully acknowledged. Two anonymous reviewers and Moujahed Al-Husseini are also acknowledged for their very valuable comments that improved the quality of the text and contents of the Cycle Chart.

APPENDIX

The Appendix includes figures and brief descriptions of some of the stratigraphic sections utilized to interpret sequence boundaries and system tracts in various segments of the stratigraphic column. These have been selected (from a larger number considered for this synthesis) to exemplify the process of building the Phanerozoic onlap patterns (and their derivative sea-level curves) as plotted on the Cycle Chart (see also section on "Stratigraphic Sections used for Detailed Interpretations"). Sequence boundaries (SBs) and maximum flooding surfaces (MFSs) are plotted alongside existing interpretations by the authors of the published sections. Occasionally, the existing interpretations are modified and reasons are given for the changes. The methodology of construction of regional onlap and sea-level curves are also discussed in the main body of the text.

For consistency, most of the figures (ascribed to various authors mentioned below) included in the Appendix to exemplify our methodology are taken from the versions published by Sharland et al. (2001) who have already to some extent modified some of the original figures. These authors include: Boucot et al. (1985), Loutfi and Abdel Sattar (1987), Wilson (1985), Hughes Clark (1988), Droste (1990), Yousif and Nouman (1997), Droste (1997), Wender et al. (1998), and Al-Fares et al. (1998), Clayton et al. (2000). Five summary chronostratigraphic figures of Sharland et al. (2001), (our Figures 2, 5, 8, 10 and 12) that incorporate their major numbered MFSs, as well as the SBs and MFSs interpreted by us, are also reproduced. The location of various stratigraphic outcrop and well sections selected as examples here are shown in Figure 1.

A schematic chronostratigraphic cross-section that summarizes the Cambrian through early Silurian stratigraphy of the Arabian Platform (adapted from Sharland et al., 2001) is reproduced in Figure 2. This summary is a convenient way to envision the cycles and broad transgressions of the Platform from the northeast and the dominant lithologies associated with these wide transgressive-regressive

cycles (indicated by Sharland et al. with large arrows in the retrogradational and progradational directions). For convenience, sequence boundaries (shown as red lines in the SB/MFS columns) are placed in the middle of the identified hiatuses. However, the exact chronological position of the SBs within these intervals is uncertain (and can shift up or down).

It is also obvious from this summary that in addition to hiatuses at the SBs, large gaps also exist in the stratigraphic succession of the Platform where record of additional sequences deposited during these intervals may be missing. In glacial environments (i.e. in the late Ashgill = Hirnantian in GTS 2004) sequences are difficult to interpret, though (as in the case of fluvial incisions) SBs can be drawn at the base of the glacial valleys. In the Silurian, in the regressive successions above the Sarah and within the Qusaiba formations, several higher-order sequences (representing fourth-order cycles of a few 100 ky duration) can be identified. In the Cambrian through early Silurian interval depicted by this summary figure, thirteen major SBs are indicated by the presence of major hiatal surfaces, and nine additional SBs are interpreted (eight of those in the Ashgill are higher-order cycles mentioned above).

The Ara Group of Oman as seen in the Birba-1 well (Figure 3) represents a late Proterozoic through Early Cambrian section (after Amthor et al., 2003) with the lowermost major MFS (Cm10 at 538 Ma according to GTS 2004) that occurs within a carbonate stringer in this largely evaporitic environment. In such environments, SBs can be placed at the top of each evaporitic (desiccation) cycle. Thus, in addition to the major hiatus at 306 Ma, six additional SBs can be identified in this section. Intervening MFSs are normally placed within carbonate or shale intervals, especially where they span relatively high gamma-ray values on the e-logs (though such a relationship may not always hold in pure carbonate environments).

Droste (1997) has summarized the Cambrian through early Silurian lithostratigraphy of the Haima Supergroup of Oman (Figure 4). Here SBs can be placed at the prominent hiatal surfaces or interpreted above regressive units, and intervening MFSs can be placed within shale-rich intervals. Seven major MFSs have been identified by Sharland et al. (2001) in this interval (numbered Cm20–S10 and reassigned ages according to GTS 2004). It should be noted, however, that these cycles represent broad, second-order sequences (each of which may, when seen in more detail, comprise several third-order sequences)

Silurian through early Carboniferous stratigraphy (up to the initiation of the Hercynian Orogeny) is summarized in the chronostratigraphic cross-section of Figure 5 (after Sharland et al., 2001). Sharland et al. identified several broad transgressive-regressive cycles (indicated by large retrogradational and progradational arrows). Prominent hiatuses represent major SBs (where the record of additional sequences may be missing). The record of higher-order cycles (in the Qusaiba above and below the MFS S10) is repeated here.

The next figure (Figure 6) shows the Early Devonian of the Jauf Formation in northwest Saudi Arabia (after Boucot et al., 1985) and the SBs and MFSs interpreted in this section. SBs are placed at the top of the regressive units. In the Pragian through Emsian interval nine SBs have been interpreted that most likely represent third-order and/or higher-order cycles. The MFSs interpreted by Sharland et al.'s (D10 and D20 and reassigned ages according to GTS 2004) and those interpreted here (within the marine shale units) are also shown.

The latest Devonian to early Carboniferous interval is exemplified by the Abu Safah-29 well (Figure 7) from the northern Arabian Gulf (after Clayton et al., 2000). Sharland et al. (2001) have identified a single major MFS (C10) in this section which has been moved slightly lower to be centered within the high gamma-ray shale interval. Several higher-order cycles can be identified within the upper Jubah and Berwath formations.

The events during the main Hercynian Orogeny are responsible for the non-deposition and/or removal of over 20 my record of sedimentation on the Arabian Platform (spanning the middle and late Carboniferous) that was followed by a widespread period of glaciation (sea-level lowstand) characterized by glacial and fluvio-glacial incision on the Platform. Figure 8 shows a chronostratigraphic cross-section of the post-Hercynian Permian to Early Triassic interval (after

Sharland et al., 2001). Earliest Permian (Unayzah B) interval is characterized by stacked fluvio-glacial valley fills. The incision of each generation of valleys may be seen as a discrete sequence boundary (MFSs can not be interpreted in such environments). The later early Permian (Unayzah A) is also typified by stacked incised valley fills, which may also represent higher-order cycles. Within the Permian eleven SBs can be identified but only a few MFSs can be picked. In the late Permian and Scythian (Khuff A-C) carbonate sedimentation begins to dominate and discrete sedimentary cycles become discernable once again. Major MFSs P10 through Tr30 have been reassigned ages according to GTS 2004 in this summary figure.

A lithostratigraphic cross-section (Figure 9) for the Permian-Early Triassic interval from the Unayzah reservoir (Unayzah and Khuff formations overlying the pre-Unayzah unconformity and the Silurian Qusaiba Member) in the Ghawar area of eastern Saudi Arabia is reproduced here (after Wender et al., 1998). Several third-order cycles can be identified in the Unayzah and are placed near the top of the regressive units. Higher-order cycles are seen in the Khuff Formation where the tops of desiccation events mark the SBs. Ages of the 2 major hiatal events have been reassigned ages according to GTS 2004.

Figure 10 shows a summary chronostratigraphic cross-section that spans the Triassic interval (after Sharland et al., 2001). Most of the SBs occur at hiatal surfaces where there are prominent gaps in sedimentation. Intervening MFSs of Sharland et al. (Tr10–Tr80) and those interpreted here are also shown. Sharland et al. identified eight broad transgressive-regressive cycles in the Triassic of the Platform (indicated by large retrogradational and progradational arrows). Here we interpret eleven complete (third-order) cycles within the Triassic interval. The close of the Triassic saw a long-term drop of sea-level that lasted nearly 20 my into the Jurassic and is characterized by lack of sedimentation and/or erosion on the Platform. The major MFSs have been reassigned ages according to GTS 2004.

The Triassic succession is exemplified by the stratigraphic section of well Umm Shaif-116 off Abu Dhabi (Figure 11). Sharland et al.'s major MFSs Tr30 and Tr50–Tr70 are recoded here (and shown with reassigned ages according to GTS 2004). In addition, several minor MFSs as well as SBs are also interpreted in this composite section (after Loufti and Abdel Sattar, 1987, fide Sharland et al., 2001).

A composite chronostratigraphic summary (Figure 12) that spans the Jurassic through Cretaceous interval is adapted from Sharland et al. (2001). Major Jurassic and Cretaceous MFSs of Sharland et al. (J10–J110 and K10–K150 with reassigned ages according to GTS 2004) and additional MFSs as well as intervening SBs interpreted here are also shown. As mentioned earlier, a long-term global sea-level fall that began near the end of Triassic (late Norian) continued into the Early Jurassic (Hettangian through Pliensbachian) causing extensive erosion and/or non-deposition on the Platform and is represented by a major sedimentary gap.

A Jurassic lithostratigraphic section from Well Minagish-27 of Kuwait (after Yousif and Nouman, 1997) is reproduced in Figure 13 together with the sequence stratigraphic interpretations. Higher-order cycles are interpreted in the lower Marrat Formation (SBs are picked at the end of the desiccation cycles), topped by the major MFS (J10) of Sharland et al. (2001). Ages of J10 and other MFSs have been modified according to GTS 2004

Figure 14 shows a Middle to Late Jurassic lithostratigraphic section from Qatar (after Droste, 1990) together with the sequence stratigraphic interpretations. These include the Sharland et al.'s major MFSs (J20–J100 with reassigned ages according to GTS 2004) and the intervening SBs interpreted by us. In these carbonate sequences the SBs generally occur very close to the overlying MFSs. The stratigraphic section from the Qatif field of eastern Saudi Arabia (Figure 15) also exemplifies the Middle to Late Jurassic of the region (after Wilson, 1985). Sharland et al.'s J40 through J110 MFSs are recorded here. Three higher-order cycles are interpreted below MFS J80 and five above J100. In the latter, MFSs can not be easily interpreted but most likely occur within the limestone units.

In Well "F" from Kuwait offshore (Figures 16-18) a nearly complete latest Jurassic through Cretaceous interval is represented (after Al-Fares et al., 1998). Figure 16 exemplifies the older part of Early Cretaceous interval. Sharland et al.'s major MFSs (J110 through K40 with reassigned ages according to

continued on page 148

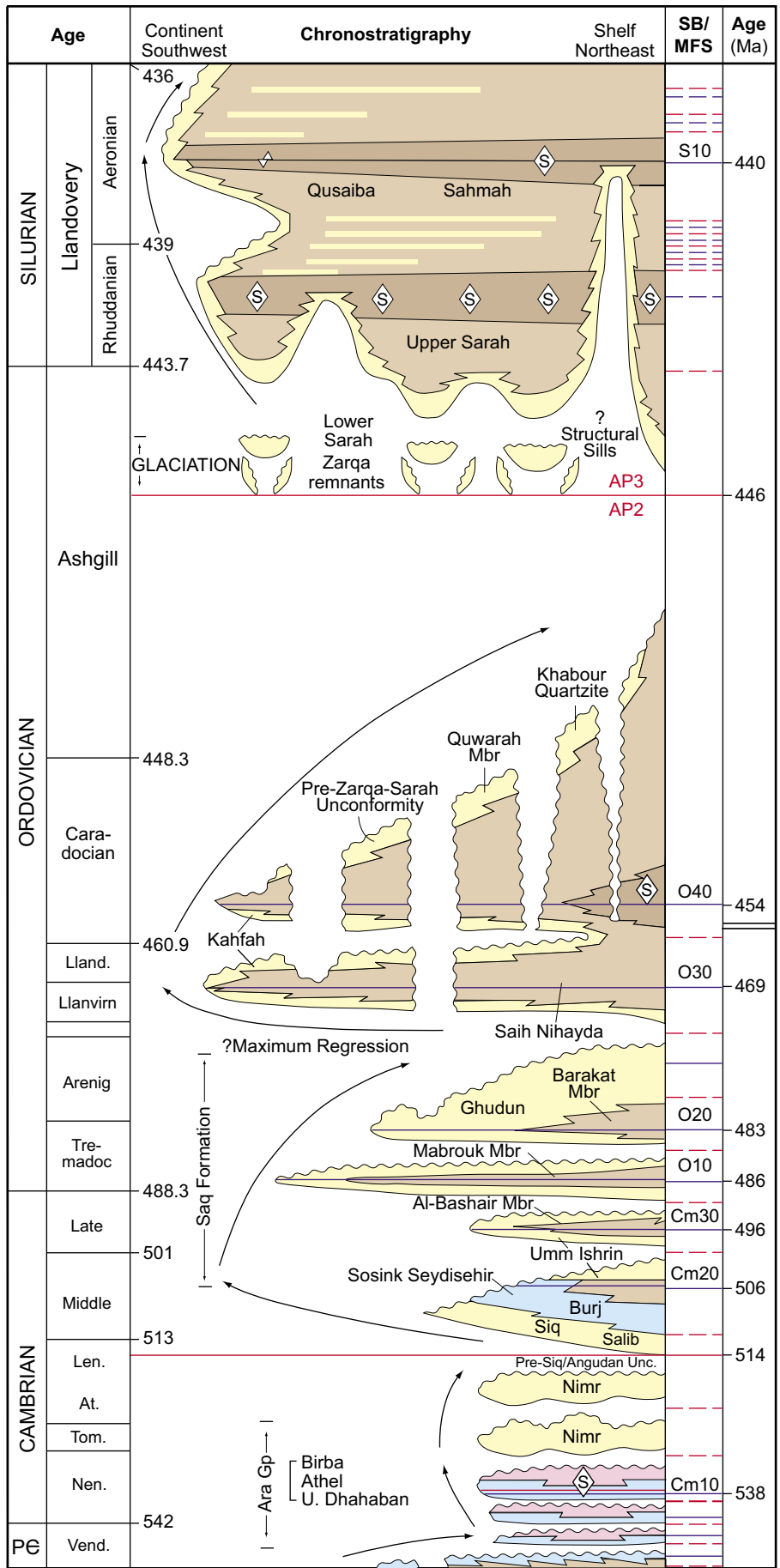


Figure 2: Schematic chronostratigraphic summary of the Cambrian through early Silurian interval after Sharland et al. (2001) with interpreted sequence boundaries (SBs) and maximum flooding surfaces (MFSs). Age column is not to scale and assigned ages are according to GTS 2004. MFSs include both those interpreted by Sharland et al. (numbered Cm10 through S10) and those interpreted here (unnumbered). SBs are shown as dashed red lines and MFSs as blue lines. Broad transgressive-regressive cycles as interpreted by Sharland et al. are shown with retrogradational and progradational arrows. Symbol "S" on some of the MFSs indicates the presence of oil-prone source rock at this level. [The higher-order cycles interpreted within the regressive units above Sarah and within the Qusaiba Formation are most likely fourth-order cycles].

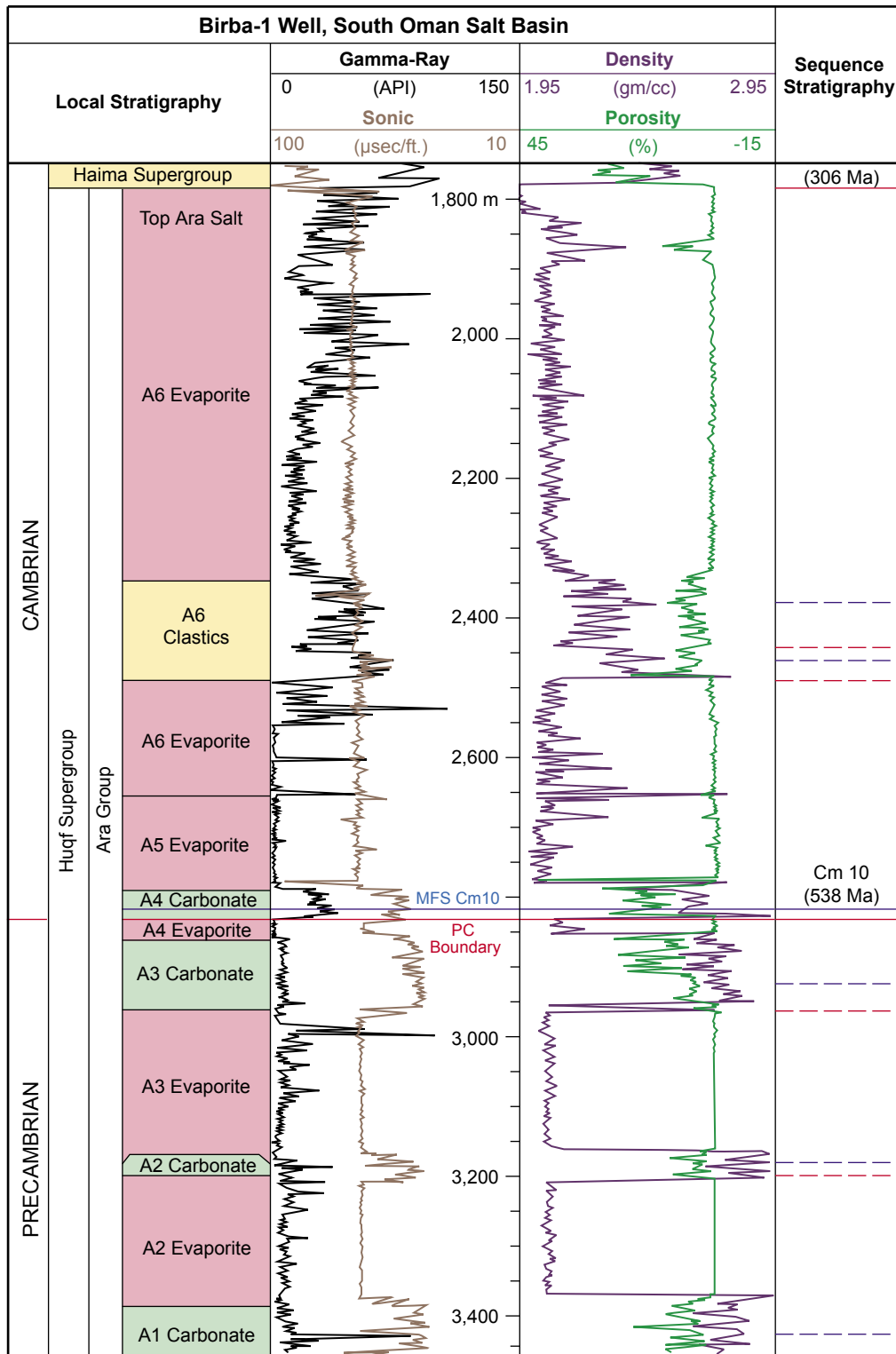


Figure 3: Lithostratigraphic section of the late Proterozoic to Early Cambrian Ara Formation as recorded in the Birba-1 well in Oman (after Amthor et al., 2003; Al-Husseini et al., 2003). The single major MFS (Cm10 with reassigned ages according to GTS 2004) in the Early Cambrian interpreted by Sharland et al. and other MFSs and SBs in the upper Ara Group interpreted here are shown. SBs are placed at the top of the desiccation events.

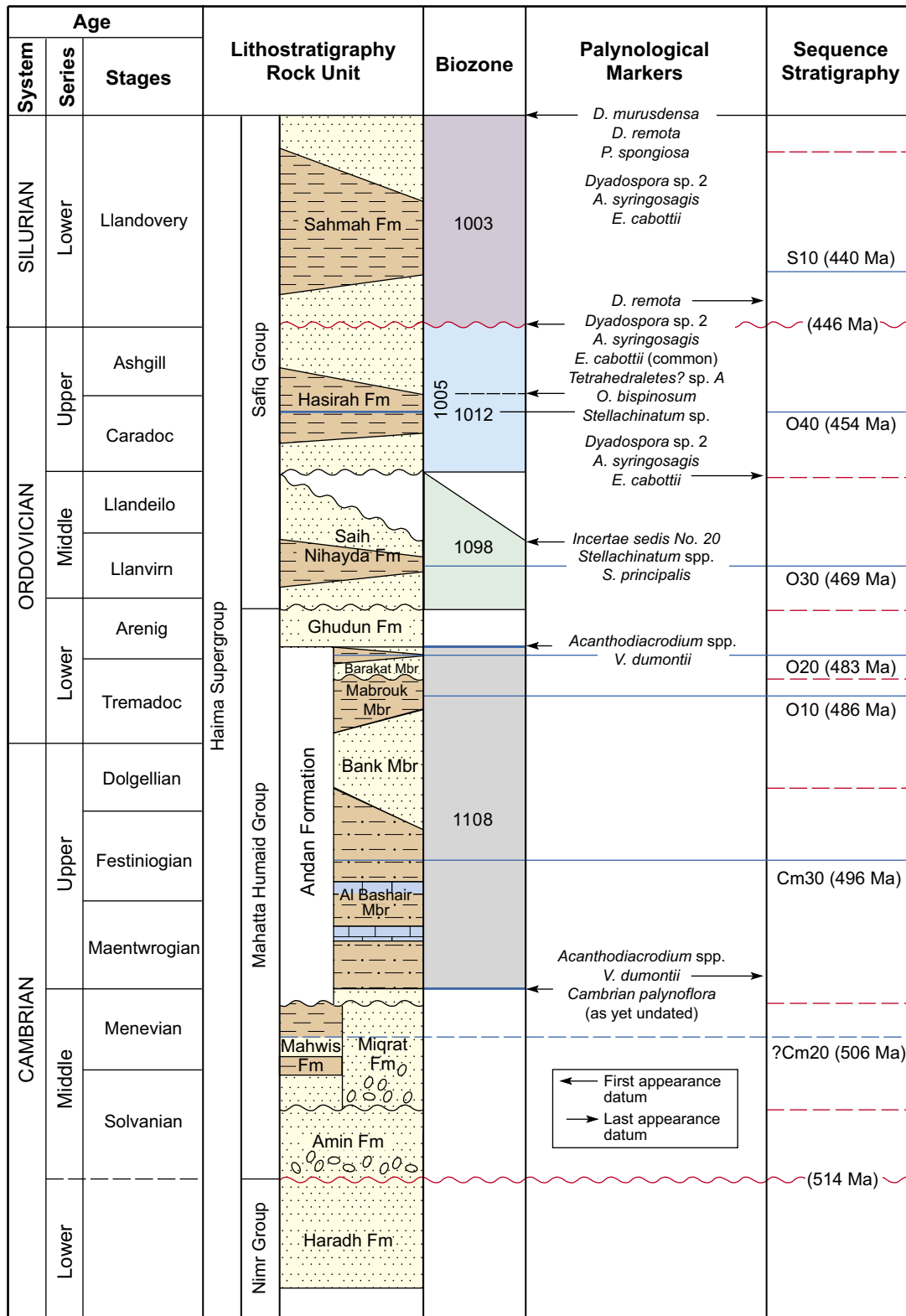


Figure 4: A schematic lithostratigraphic section of the Cambrian through early Silurian interval of the Haima Supergroup of Oman (after Droste, 1997, fide Sharland et al., 2001). Sharland et al.'s interpreted MFSs (numbered Cm20? through S10 with reassigned ages according to GTS 2004) and SBs and MFSs interpreted here are shown. For some cycles MFSs are not recognizable and are not interpreted.

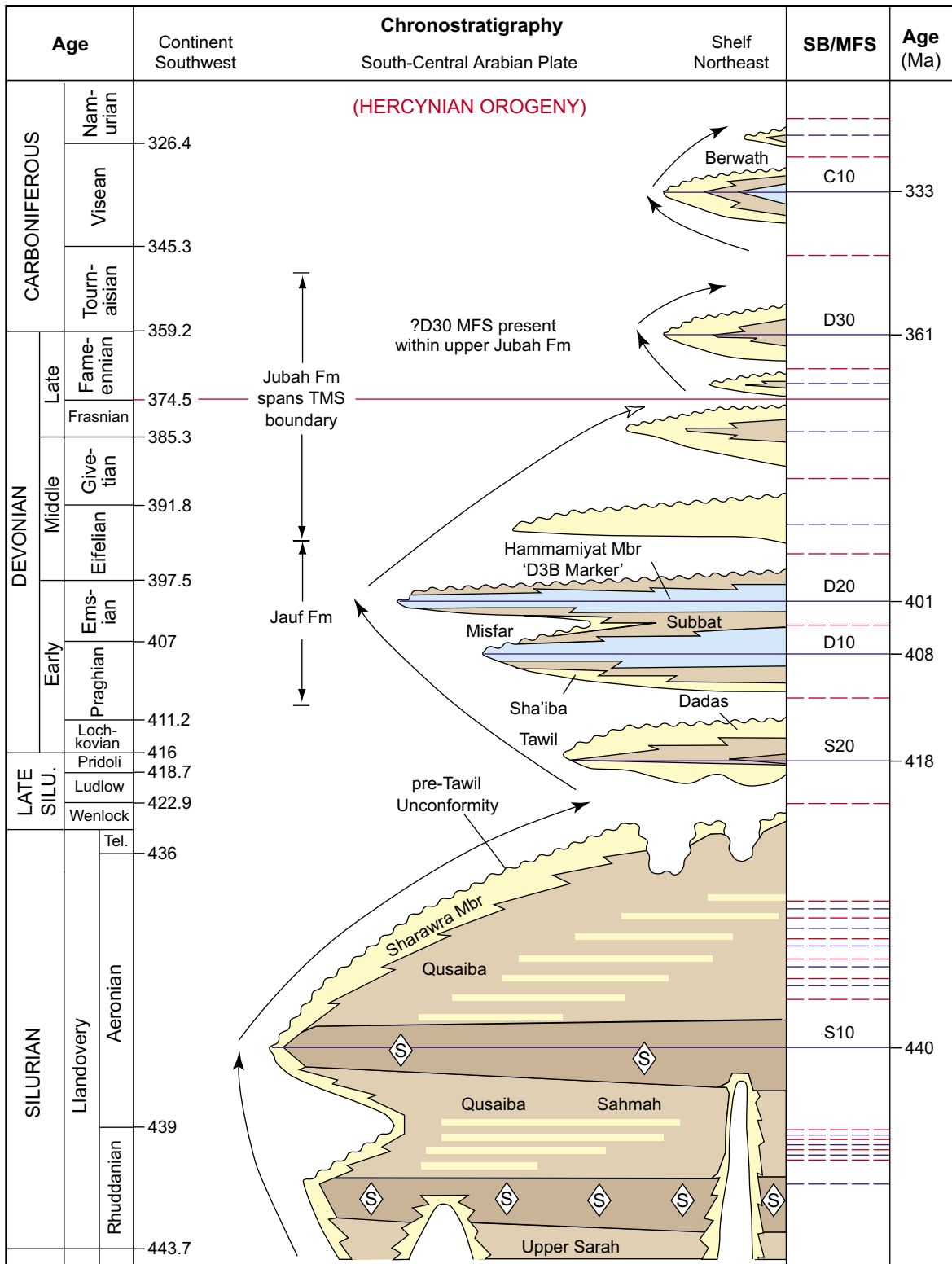


Figure 5: Schematic chronostratigraphic summary of Silurian through early Carboniferous interval after Sharland et al. (2001) with interpreted SBs and MFSs. Age column is not to scale and assigned ages are according to GTS 2004. MFSs include both those interpreted by Sharland et al. (numbered S10 through C10) and those interpreted here (unnumbered). SBs are shown as dashed red lines and MFSs as blue lines. Broad transgressive-regressive cycles as interpreted by Sharland et al. are shown with retrogradational and progradational arrows. [The higher-order cycles interpreted within the regressive units above Sarah and within the Qusaiba Formation are most likely fourth-order cycles].

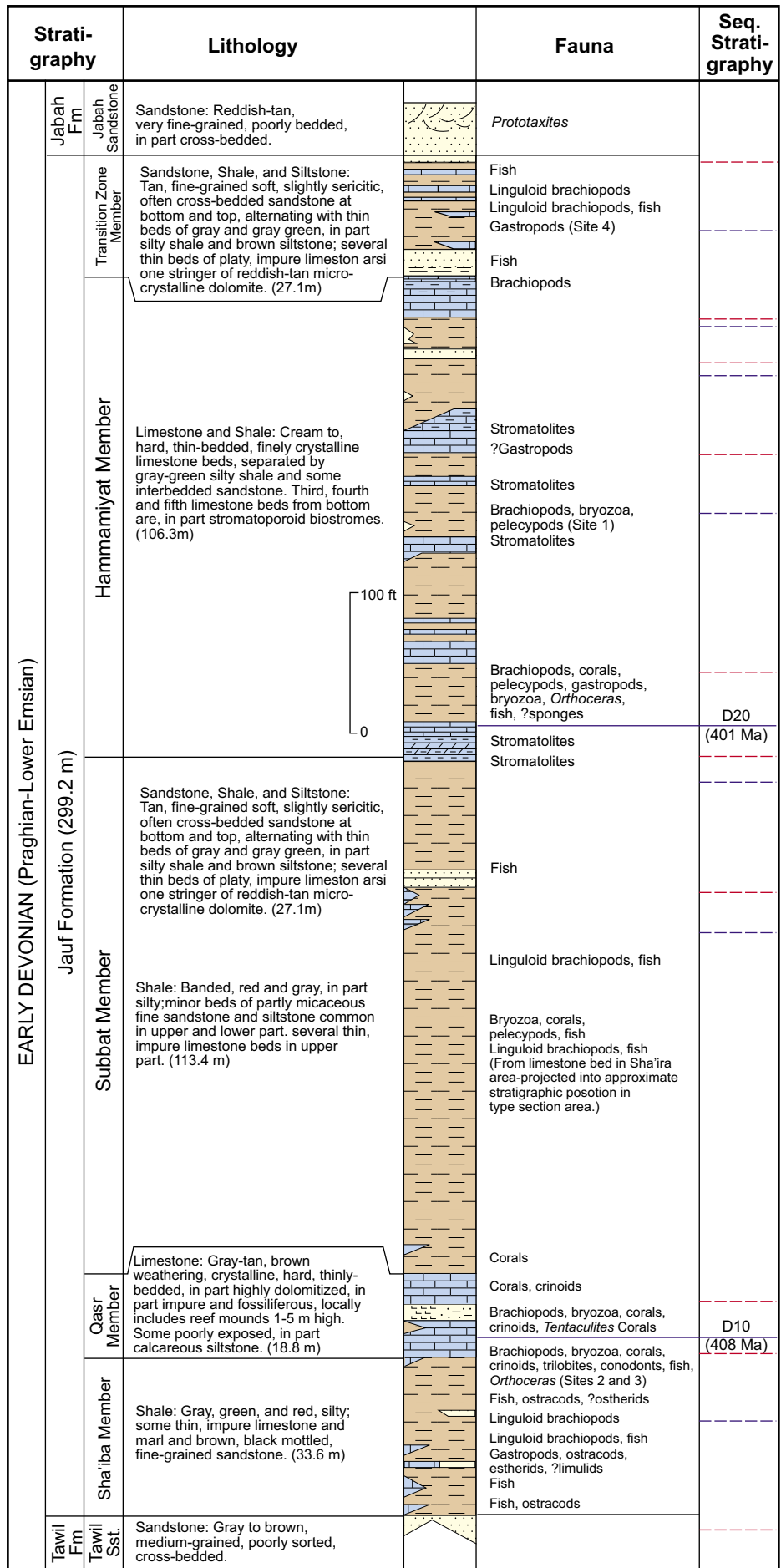


Figure 6: A generalized lithostratigraphic section spanning early Devonian (Praghan-early Emsian) of the Jauf Formation of northwestern Saudi Arabian (after Boucot et al., 1985, as modified by Sharland et al., 2001). The two major MFSs of Sharland et al. (D10 and D20 with reassigned ages according to GTS 2004) and SBs and MFSs as interpreted here are shown.

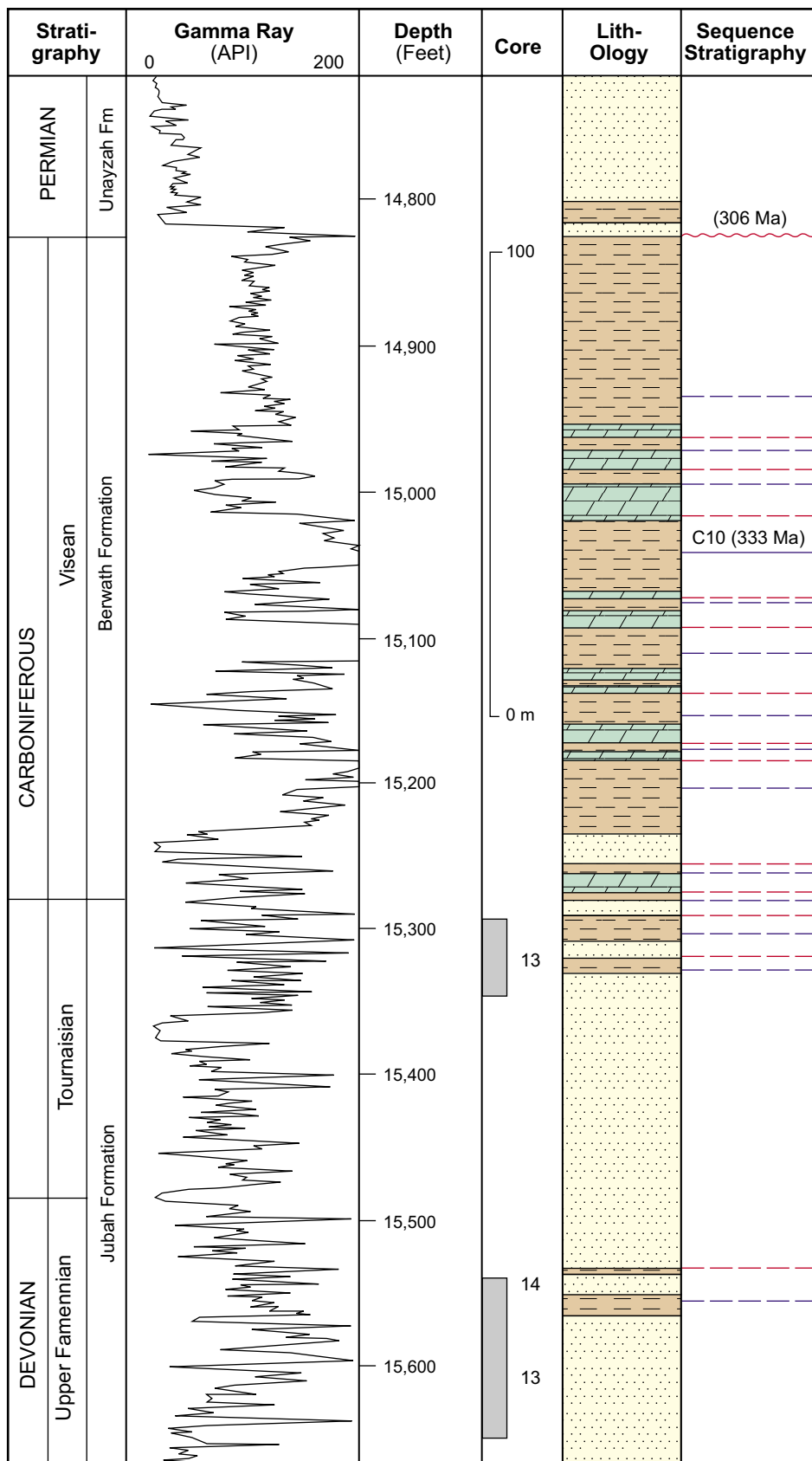


Figure 7: The lithostratigraphic section of the late Devonian through early Carboniferous interval (Jubah and Berwath formations) of Well Abu Safah-29 in the northern Gulf area (after Clayton et al., 2000, fide Sharland et al., 2001). A single major MFS of Sharland et al. and MFSs and SBs interpreted here are shown. Note that C10 has been moved slightly lower here to coincide with the gamma-ray peak. Numerous higher-order (fourth-order) cycles are also interpreted.

continued from page 141

GTS 2004) are shown together with the intervening SBs and additional cycles identified here. Cycles typically occur in this interval as large limestone-shale couplets and SBs are picked at the top of the regressive units. The middle part of this well (Figure 17) spans the younger Early Cretaceous interval (Sharland's MFS K30-K40 are repeated, and K50 through K100 with reassigned ages according to GTS 2004 are also shown). Minor cycles are also identified in this dominantly siliciclastic interval. Note that Sharland et al.'s K60 and K70 have been moved slightly (higher and lower, respectively) to center within the organic-rich beds. The upper part of Well F spans the Albian-Cenomanian interval (Figure 18) and once again becomes dominantly carbonate, showing large limestone-shale couplets that represent sequence cycles.

We have selected the section from the Baldi-1 Well from Oman to exemplify the Paleogene of the Platform (Figure 19, after Hughes Clarke, 1988). Although much of the Paleocene-Early Eocene is dominantly limestone and interpreting cycles based on log-response is largely conjectural, the younger part of Early Eocene does show several evaporitic events allowing cyclic interpretations. Sharland et al.'s Pg10 MFS is shown near a gamma-ray peak on the e-log and Pg20 MFS is picked at an organic-rich shale event with reassigned ages according to GTS 2004. continued on page 157

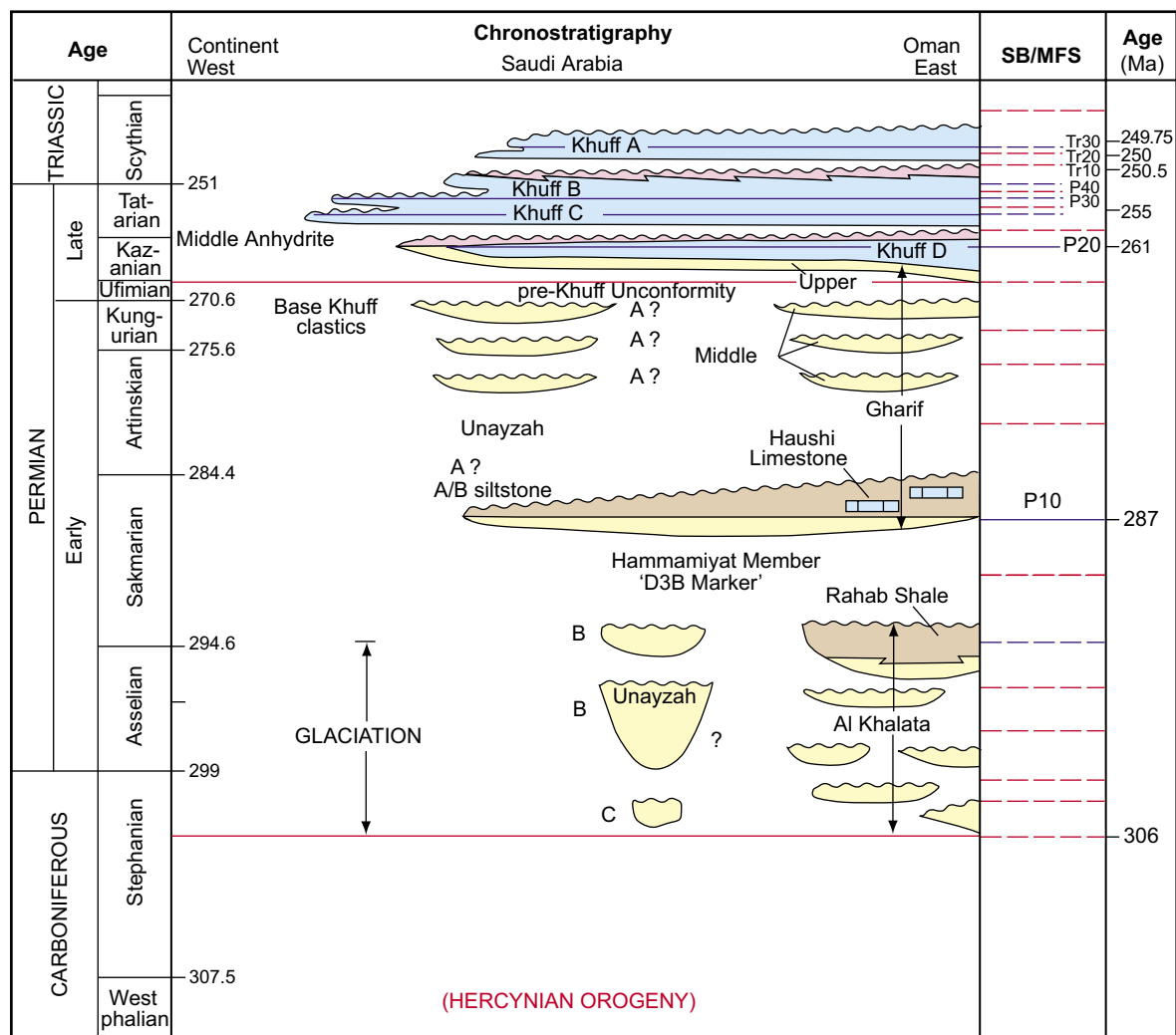


Figure 8: Schematic chronostratigraphic summary of Permian through earliest Triassic interval after Sharland et al. (2001) with interpreted SBs and MFSs. Age column is not to scale and assigned ages are according to GTS 2004. MFSs include both those interpreted by Sharland et al. (numbered P10 through Tr30) and those interpreted here (unnumbered). The latest Carboniferous-earliest Permian interval is characterized by glaciation on the Platform and is associated with fluvio-glacial incised valleys. Sequence stratigraphic interpretations are difficult in such environments, however, SBs can be drawn at the bases of glacially and fluvially incised valleys.

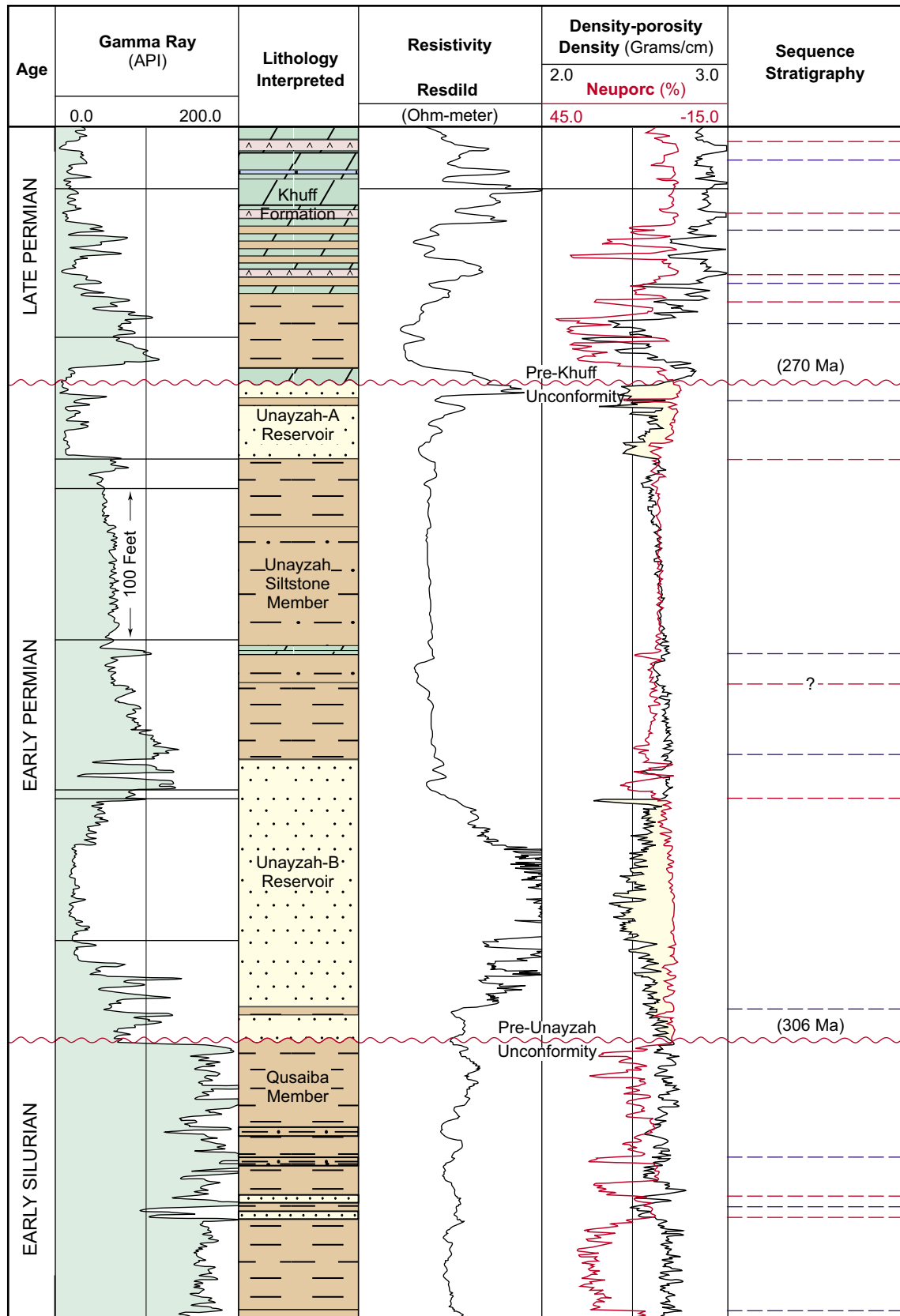


Figure 9: A schematic lithostratigraphic section of the Permian Unayzah through Khuff formations of the Ghawar area, eastern Saudi Arabia (after Wender et al., 1998) showing interpreted SBs and MFSs. In the Khuff Formation SBs are placed at the desiccation events.

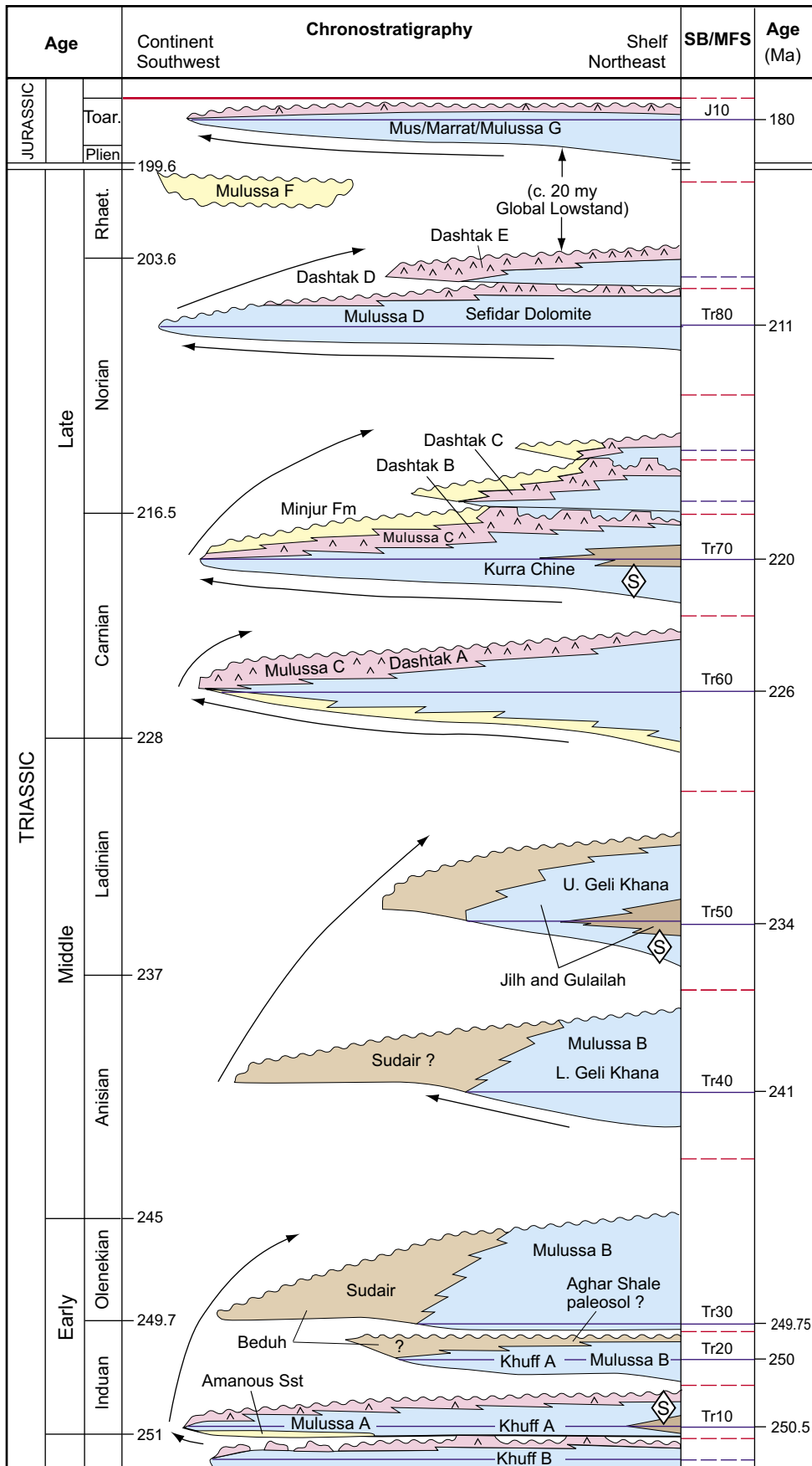


Figure 10: Schematic chronostratigraphic summary of Triassic-earliest Jurassic interval after Sharland et al. (2001) with interpreted SBs and MFSs. Age column is not to scale and assigned ages are according to GTS 2004. MFSs include both those interpreted by Sharland et al. (numbered Tr10 through J10) and those interpreted here (unnumbered). Broad transgressive-regressive cycles as interpreted by Sharland et al. are shown with retrogradational and progradational arrows.

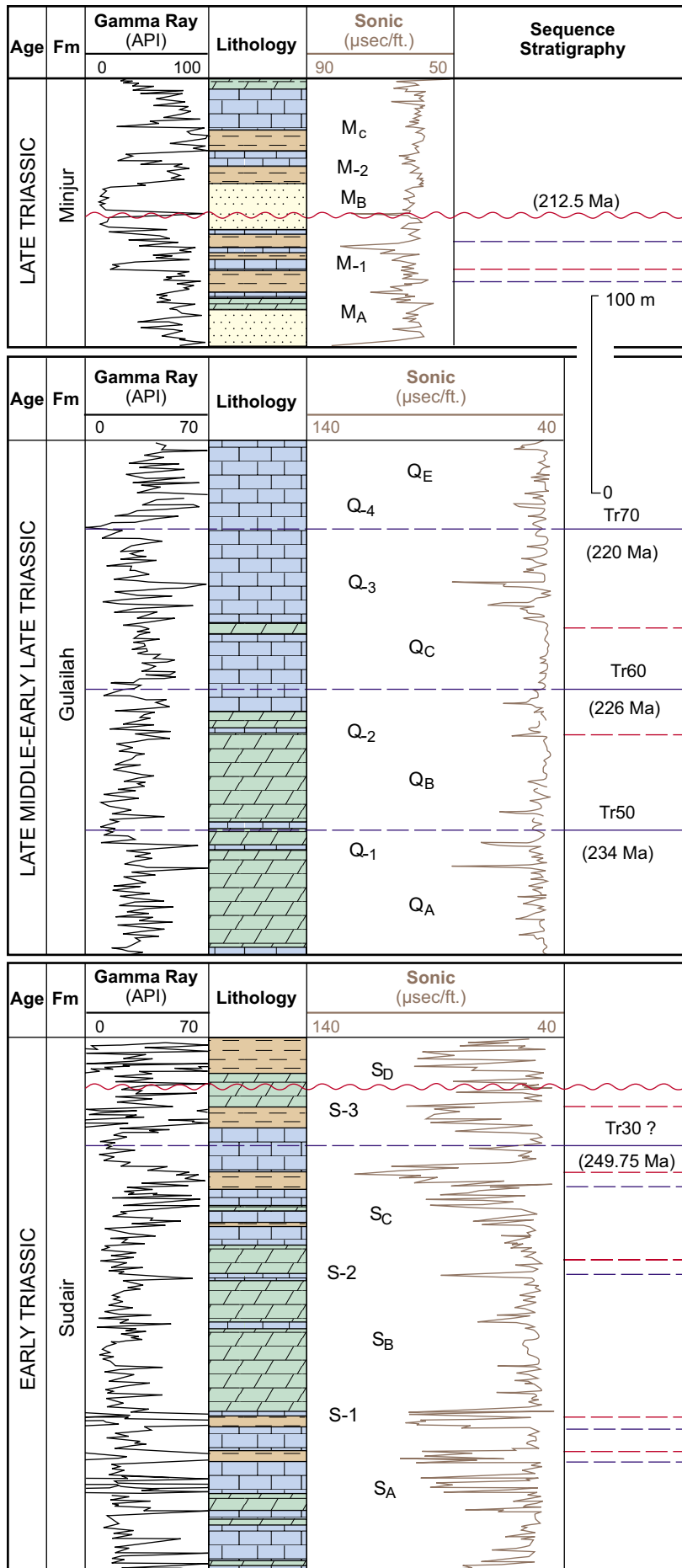


Figure 11: A lithostratigraphic section of the Triassic succession in the Umm Shaif-116 well of Abu Dhabi, Greater Gulf area (after Loutfi and Abdel Sattar, 1987, fide Sharland et al., 2001). Sharland et al.'s major MFSs (numbered Tr30-Tr70 with reassigned ages according to GTS 2004) as well as those interpreted here (unnumbered) and SBs are shown.

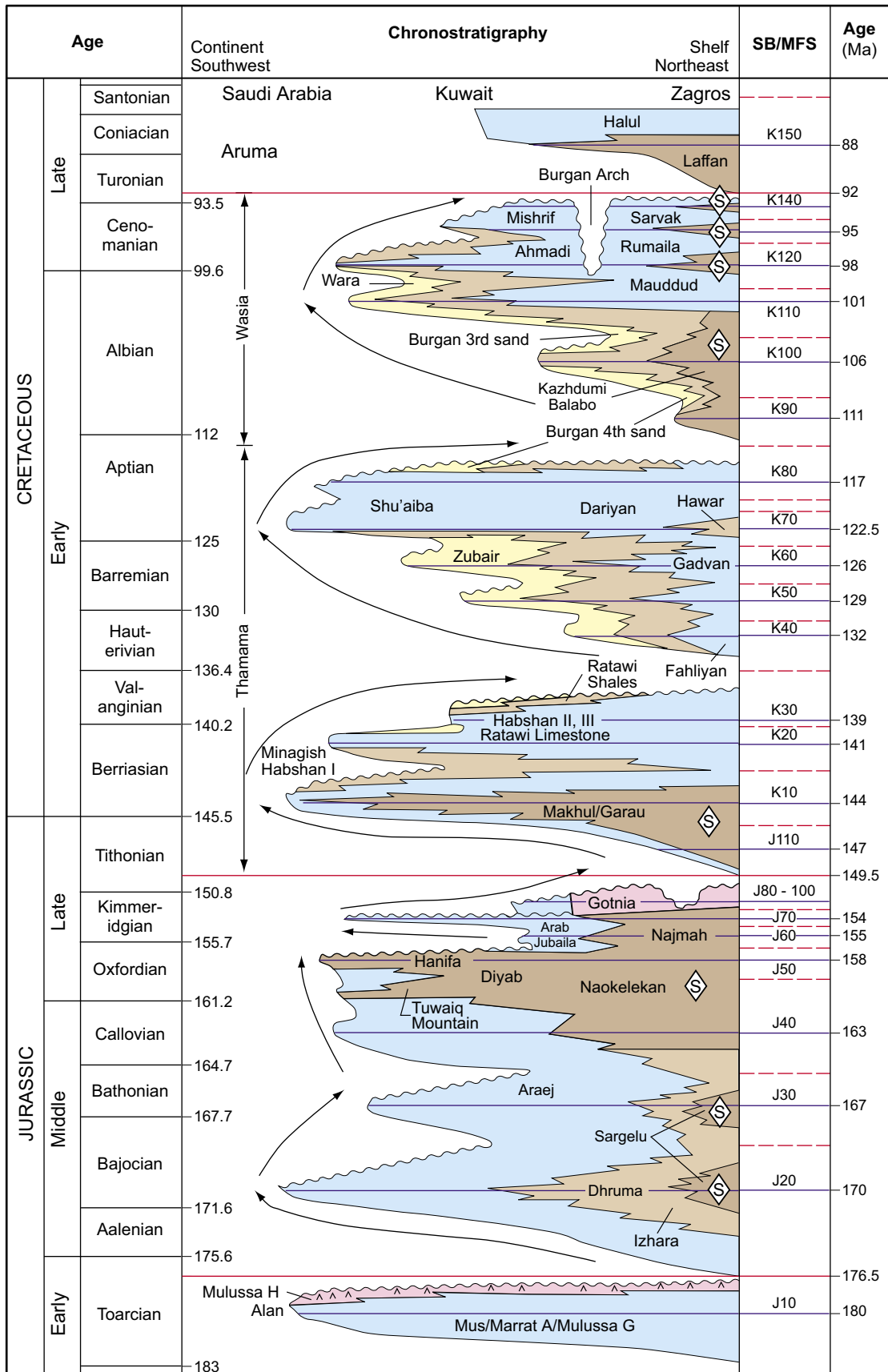


Figure 12: Schematic chronostratigraphic summary of early Jurassic-Cretaceous interval after Sharland et al. (2001) with interpreted SBs and MFSs. Age column is not to scale and assigned ages are according to GTS 2004. MFSs include both those interpreted by Sharland et al. (numbered J10 through K150) and those interpreted here (unnumbered). SBs are shown as dashed red lines and MFSs as blue lines. Broad transgressive-regressive cycles as interpreted by Sharland et al. are shown with retrogradational and progradational arrows.

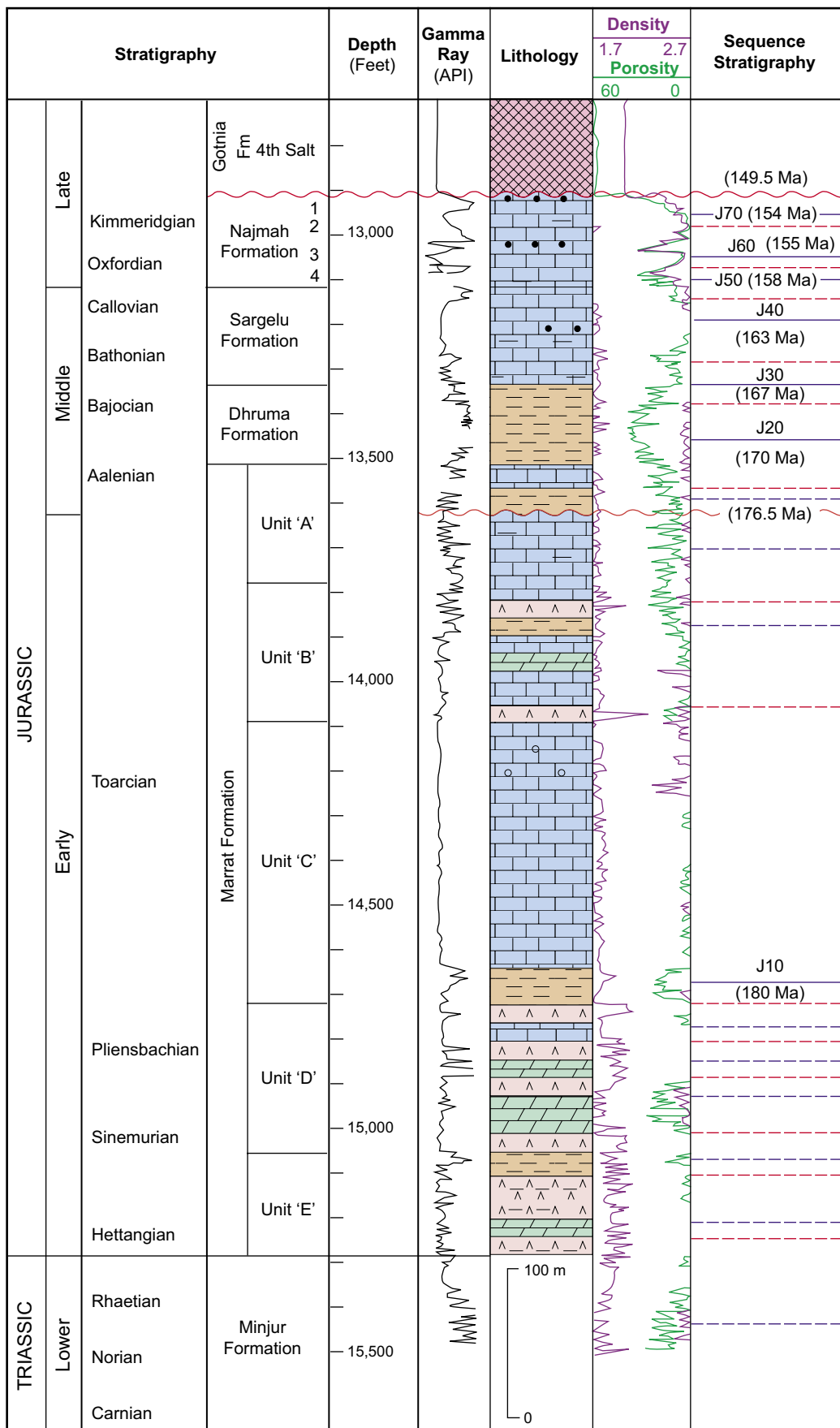


Figure 13: A lithostratigraphic section for the early-middle Jurassic interval from well Minagish-27, Kuwait (after Yousif and Nouman, 1997 fide Sharland et al., 2001). Major MFSs of Sharland et al. (numbered J10-J60) and those interpreted here (unnumbered) as well as intervening SBs are shown. Stratigraphic ages in the right column have been reassigned according GTS 2004.

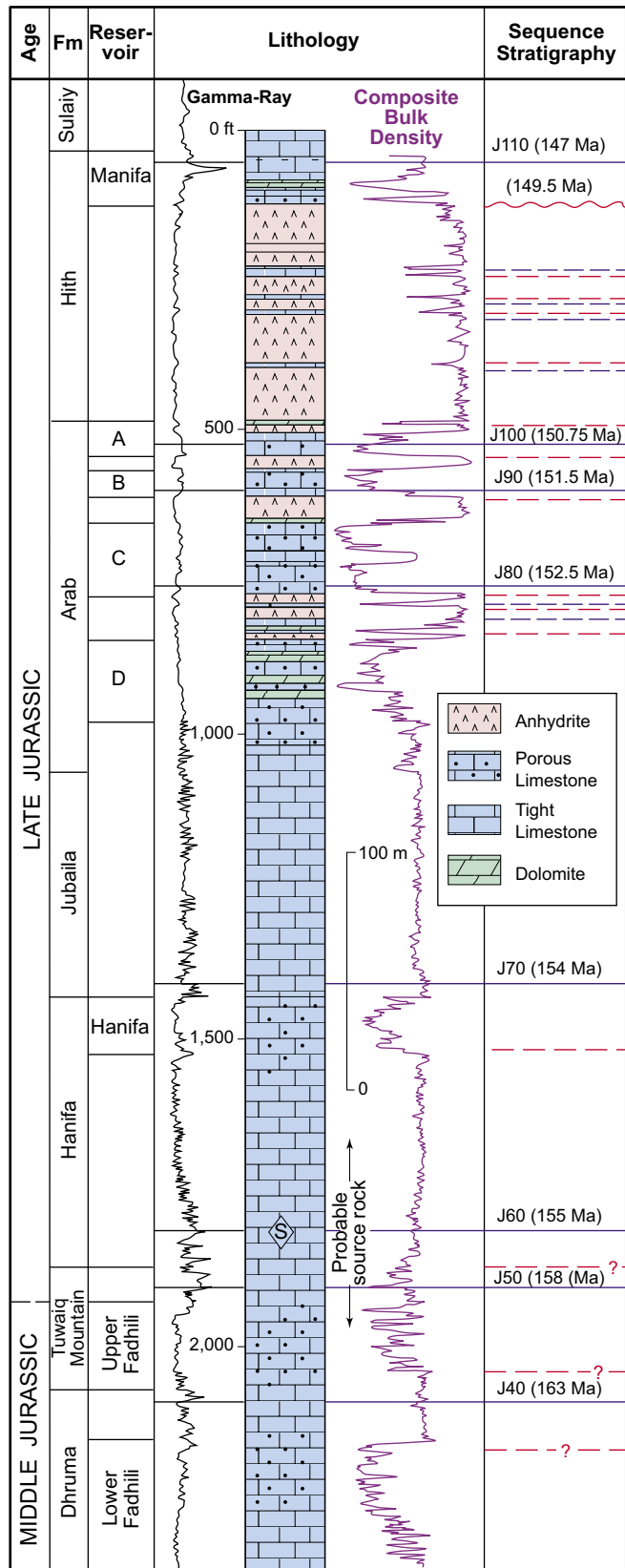
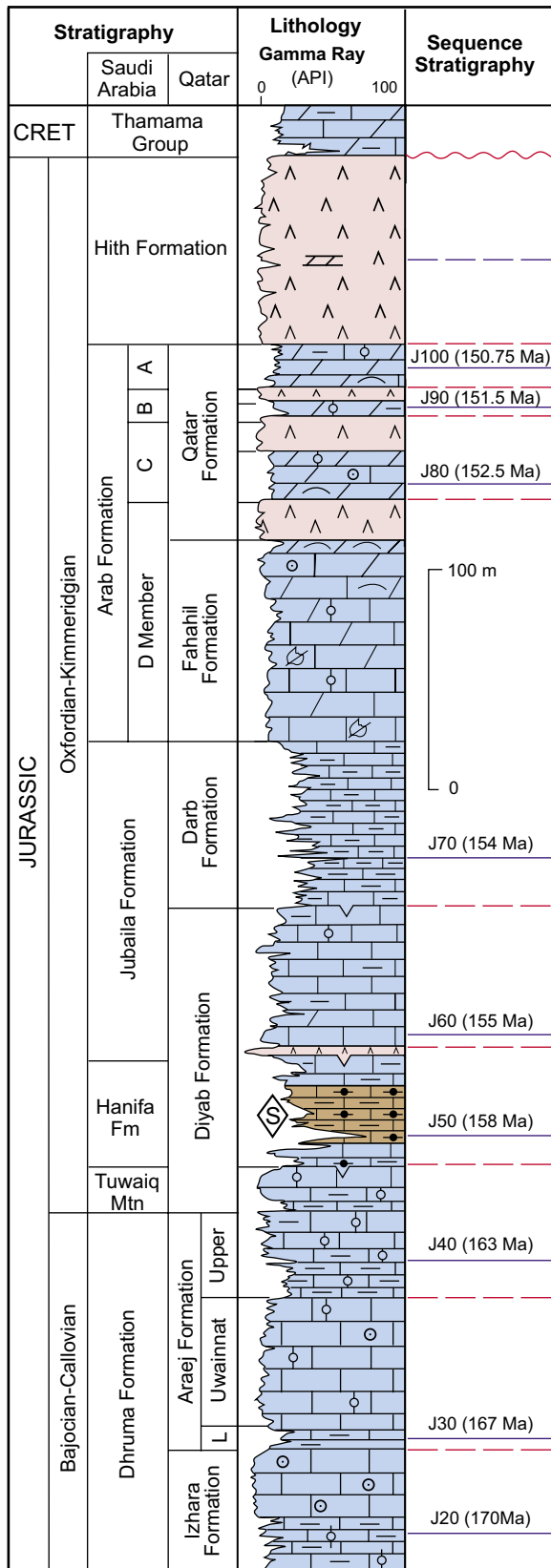


Figure 14 (left): A lithostratigraphic section for mid to late Jurassic interval of Qatar (after Droste, 1990, fide Sharland et al.'s, 2001). Both Sharland et al.'s major MFSs (J20–J100 with reassigned ages according to GTS 2004) and those interpreted here as well as intervening interpreted SBs are shown.

Figure 15 (right): A lithostratigraphic section of the mid to late Jurassic of Qatif field of eastern Saudi Arabia (after Wilson, 1985, fide Sharland et al., 2001), showing Sharland et al.'s major MFSs (J40–J110 with reassigned ages according to GTS 2004) and those interpreted here as well as the intervening SBs. In the Arab and Hith formations the SBs are placed at the top of the desiccation events. However, the position of the MFSs within these cycles are not easily assigned though they may occur within the limestone units.

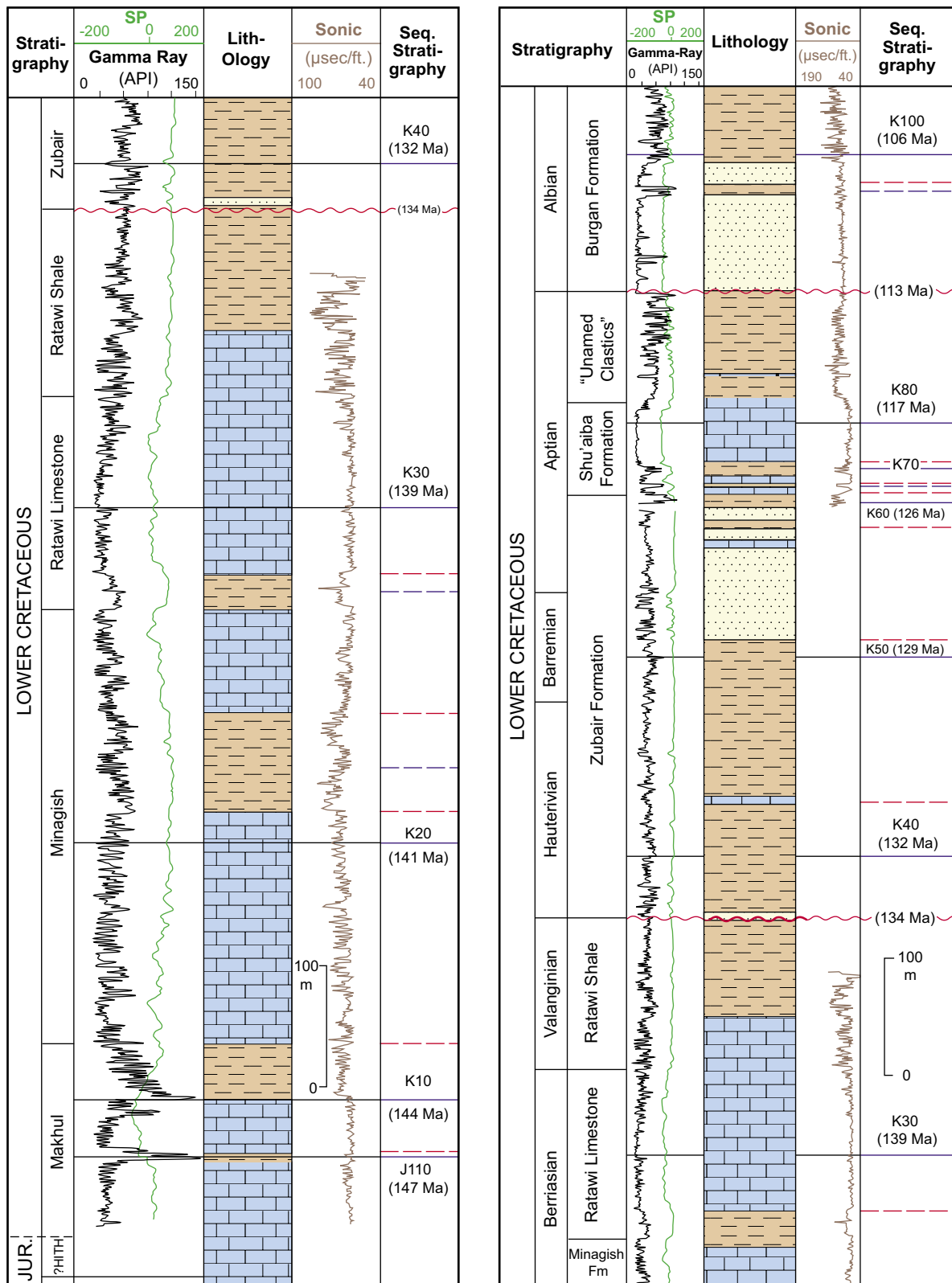


Figure 16 (left): A lithostratigraphic section of the early Cretaceous interval of Well F, Kuwait offshore in the Arabian Gulf (after Al-Fares et al., 1998, *vide* Sharland et al., 2001). Numbered MFSs (J110-K40 with reassigned ages according to GTS 2004) are after Sharland et al. and those interpreted here as well the intervening SBs are unnumbered.

Figure 17 (right): A lithostratigraphic section of the early Cretaceous (Berriasian to Albian) of Well F, Kuwait offshore (after Al-Fares et al., 1998, *vide* Sharland et al., 2001). Note that the position of MFSs K60 and K70 have been moved slightly up and down, respectively, to coincide with organic-rich peaks within the shales. Numbered MFSs (K30-K100 with reassigned ages according to GTS 2004) are after Sharland et al. and those interpreted here and the intervening SBs are unnumbered.

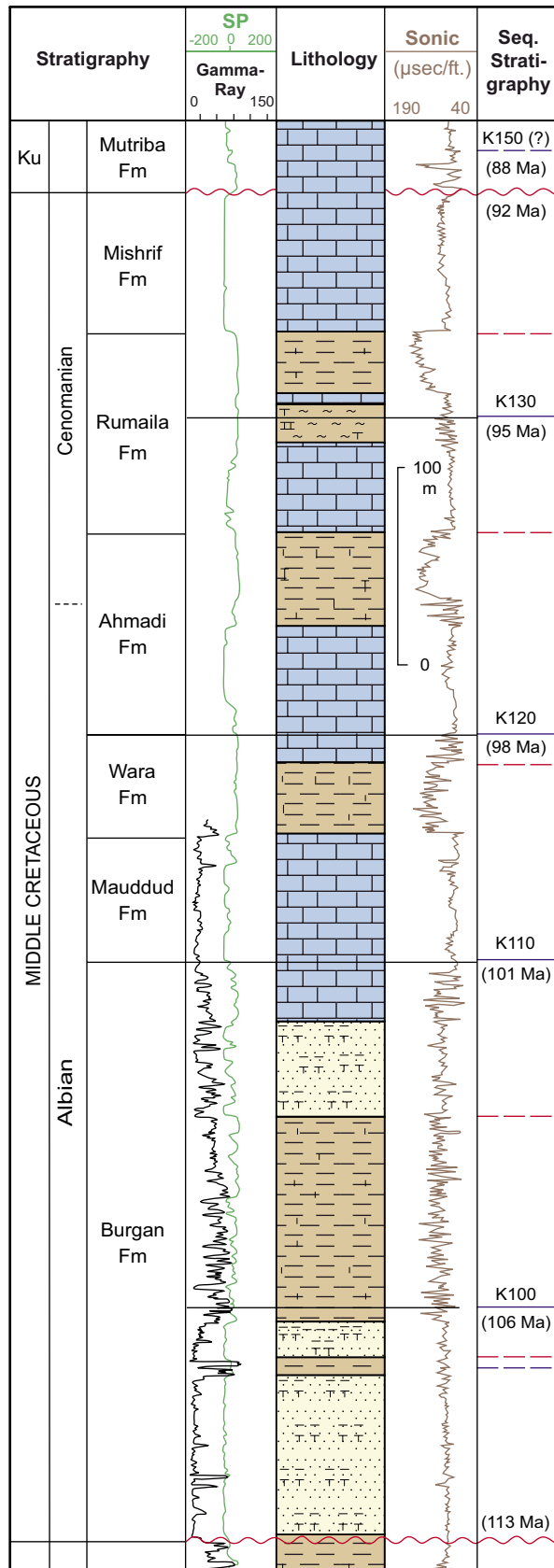


Figure 18: The mid Cretaceous (Albian-Cenomanian) interval of Well F, Kuwait offshore (after Al-Fares et al., 1998, fide Sharland et al., 2001). Numbered MFSs (K100-K130 with reassigned ages according to GTS 2004) are after Sharland et al. and those interpreted here as well the intervening SBs are unnumbered.

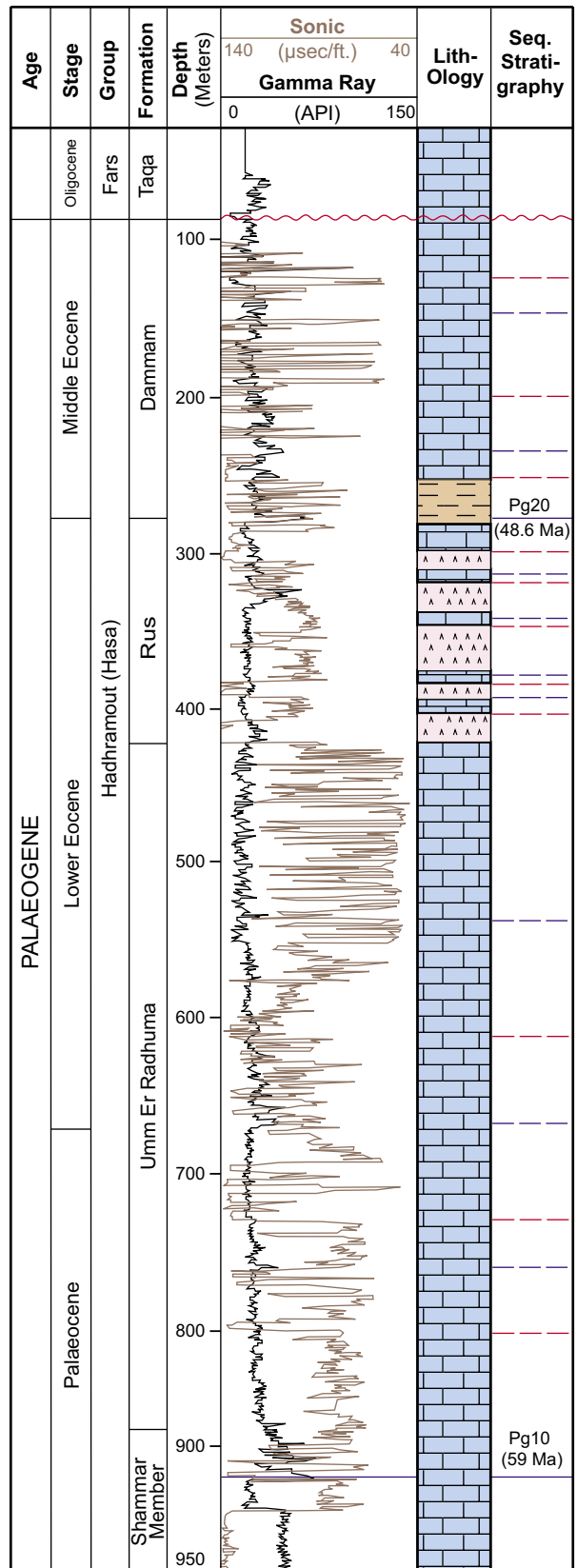


Figure 19: A lithostratigraphic section of the preserved Paleogene record of Well Baldi-1 of Oman (after Hughes Clarke, 1988, fide Sharland et al., 2001). Sharland et al.'s major MFSs are numbered (Pg10 and Pg20 with reassigned ages according to GTS 2004), while those interpreted here and the intervening SBs are unnumbered.

REFERENCES

- Al-Aswad, A.A. 1997. Stratigraphy, sedimentary environment and depositional evolution of Khuff Formation in south central Saudi Arabia. *Journal of Petroleum Geology*, v. 20, p. 307-326.
- Al-Fares, A.A., M. Bouman and P. Jeans 1998. A new look at the Middle to Lower Cretaceous stratigraphy, offshore Kuwait. *GeoArabia*, v. 3, no. 4, p. 543-560.
- Al-Husseini, M.I. 1997. Jurassic stratigraphy of western and southern Arabian Gulf. *GeoArabia*, v. 2, no. 4, p. 361-382.
- Al-Husseini, M.I. 2000. Origin of the Arabian Plate structures: Amar collision and Najd rift. *GeoArabia*, v. 5, no. 4, p. 527-54.
- Al-Husseini, M., J.E. Amthor, J. Grotzinger and J. Mattner 2003. Arabian Plate Precambrian-Cambrian boundary interpreted in Oman's Ara Group. *GeoArabia*, v. 8, no. 4, p. 578-580.
- Alsharhan, A.S. 1987. Geology and reservoir characteristics of carbonate buildup in giant Bu Hasa oil field, Abu Dhabi. *American Association of Petroleum Geologists Bulletin*, v. 71, p. 1304-1318.
- Amthor, J.E., J.P. Grotzinger, S. Schröder, S.A. Bowring, J. Ramezani, M.W. Martin and A. Matter 2003. Extinction of Cloudina and Namacalathus at the Precambrian-Cambrian boundary in Oman. *Geology*, v. 31, p. 431-434.
- Azer, S.R. and R.G. Peebles 1998. Sequence stratigraphy of the Arab A to C members and Hith Formation offshore Abu Dhabi. *GeoArabia*, v. 3, no. 2, p. 251-268.
- Aziz, S.K. and M.M.A. El-Sattar 1997. Sequence stratigraphic modeling of the Lower Thamama Group, eastern onshore Abu Dhabi. *GeoArabia*, v. 2, no. 2, p. 179-202.
- Barron, J., B. Larsen and J.G. Baldauf 1991. Evidence for late Eocene to early Oligocene Antarctic glaciation and observations on late Neogene glacial history of Antarctica: results from Leg 119. *Proceedings of the Ocean Drilling Program, Scientific Results*, v. 119, p. 869-891.
- Bartek, L.R., P.R. Vail, J.B. Anderson and M.I. Ross 1991. Effect of Cenozoic ice sheet fluctuations in Antarctica on the stratigraphic signature of Neogene. *Journal of Geophysical Research*, v. 98B, p. 6753-6778.
- Berggren, W.A., D.V. Kent, I.C.C. Swisher and M.-P. Aubry 1995. A revised geochronology and chronostratigraphy. In, W.A. Berggren, D.V. Kent, M.-P. Aubry and J. Hardenbol (Eds.), *Geochronology, Time Scales and Global Stratigraphic Correlation*. Society of Economic Paleontologists and Mineralogists Special Publication, v. 54, p. 129-212.
- Bishop, R.S. 1995. Maturation history of the Lower Paleozoic of eastern Arabian Platform. In, M.I. Al-Husseini (Ed.), *Middle East Petroleum Geosciences, GEO'94*. Gulf PetroLink, Bahrain, v. 1, p. 180-189.
- Boucot, A.J., H.A. McClure, F. Alvarez, J.R.P. Ross, D.W. Taylor, W. Struve, N.N. Savage and S. Turner 1985. New Devonian fossils from Saudi Arabia and their biogeographical affinities. *Senckenbergiana Lethaea*, v. 69, p. 535-597.
- Brannan, J., K.D. Gerdes and I.R. Newth 1997. Tectono-stratigraphic development of the Qamar Basin, eastern Yemen. *Marine and Petroleum Geology*, v. 14, p. 701-730.
- Brennan, P. 1990. Greater Burgan field. In, E.A. Beaumont and N.H. Foster (Eds.), *Structural Traps I, Treatise of Petroleum Geology, Atlas of Oil and Gas Fields*. American Association of Petroleum Geologists Bulletin, p. 103-128.
- Chaude, A.N. and J. Al-Samahiji 1995. Jurassic and Cretaceous of Bahrain: geology and petroleum habitat. In, M.I. Al-Husseini (Ed.), *Middle East Petroleum Geosciences, GEO'94*. Gulf PetroLink, Bahrain, v. 1, p. 292-305.
- Chen, Z.Q. and G.R. Shi 2003. Late Paleozoic depositional history of the Tarim basin, northwest China: an integration of biostratigraphic and lithostratigraphic constraints. *American Association of Petroleum Geologists Bulletin*, v. 87, p. 1323-1354.
- Christian, L. 1997. Cretaceous subsurface geology of the Middle East region. *GeoArabia*, v. 2, no. 3, p. 239-256.
- Clayton, G., B. Owens, S. Al-Hajri and J. Filatoff 2000. Latest Devonian and Early Carboniferous miospore assemblages from Saudi Arabia. In, S. Al-Hajri and B. Owens (Eds.), *Stratigraphic Palynology of the Paleozoic of Saudi Arabia*. *GeoArabia Special Publication 1*, Gulf PetroLink, p. 146-153.
- Droste, H.H.J. 1990. Depositional cycles and source rock development in an epeiric intra-platform basin. The Hanifa Formation of the Arabian Peninsula. *Sedimentary Geology*, v. 69, p. 281-296.
- Droste, H.H.J. 1997. Stratigraphy of the Lower Paleozoic Haima Supergroup of Oman. *GeoArabia*, v. 2, no. 4, p. 419-472.
- Eberli, G. and R.N. Ginsburg 1989. Cenozoic progradation of the northwestern Great Bahamas Bank. *Society of Economic Paleontologists and Mineralogists, Special Publication*, v. 44, p. 339-351.
- El-Bishlawy, S.H. 1985. Geology and hydrocarbon occurrence of the Khuff Formation in Abu Dhabi, UAE. *Proceedings of the 4th Society Petroleum Engineers Middle East Technical Conference*, SPE paper no. 13678, p. 601-606.

- Enay, R., Y-M. Le Nindre, C. Mangold, J. Manivit and D. Vaslet 1987. Le Jurassique d'Arabie saoudite centrale. In, R. Enay (Ed.), *Le Jurassique d'Arabie Saoudite Centrale*. Geobios, Lyon, Memoire Special, no. 9, p. 13-65.
- Evans, D.S., B.H. Bahabri and A.M. Al-Otaibi 1997. Stratigraphic trap in the Permian Unayzah Formation, central Saudi Arabia. *GeoArabia*, v. 2, no. 3, p. 259-278.
- Gorin, G.E., L.G. Racz and M.R. Walter 1982. Late Precambrian-Cambrian sediments of Huqf Group, Sultanate of Oman. *American Association of Petroleum Geologists Bulletin*, v. 66, p. 2609-2627.
- Grabowski, G.J., Jr. and I.O. Norton 1995. Tectonic controls on the stratigraphic architecture and hydrocarbon systems of the Arabian Plate. In, M.I. Al-Husseini (Ed.), *Middle Eastern Petroleum Geosciences, GEO'94*. Gulf PetroLink, Bahrain, v. 1, p. 413-430.
- Gradstein, F.M., F.P. Agterberg, J.G. Ogg and J. Hardenbol 1994. A Mesozoic time scale. *Journal of Geophysical Research*, v. 99, p. 24051-24074.
- Gradstein, F.M. and J. Ogg 1996. A Phanerozoic time scale. *Episodes*, v. 19, p. 3-5.
- Gradstein, F.M., F.P. Agterberg, J.G. Ogg, J. Hardenbol, P. van Veen, J. Teierry and Z. Huang 1994. A Mesozoic time scale. *Journal of Geophysical Research*, v. 99, p. 24051-24074.
- Gradstein, F.M., et al., 2004. A new geological time scale, with special reference to Precambrian and Neogene. *Episodes*, v. 27, no. 2, p.83-100.
- Hallam, A. 1992. *Phanerozoic Sea-level Changes*. Columbia University Press, New York, 266 pp.
- Haq, B.U. and A.M. Al-Qahtani 2002. Phanerozoic regional Cycle Chart of sea level changes for the Arabian Platform. *American Association of Petroleum Geologists, International Petroleum Conference and Exhibition, Cairo, Egypt, Abstracts*, p. A40.
- Haq, B.U., J. Hardenbol and P.R. Vail 1988. Mesozoic and Cenozoic chronostratigraphy and cycles of sea-level change. *Society of Economic Paleontologists and Mineralogists*, v. 42, p. 71-108.
- Haq, B.U. and F.W.B. van Eysinga 1998. *A geological time table*. Elsevier Science Publishers. Amsterdam, The Netherlands. Wall chart.
- Harland, W.B., R.L. Armstrong, A.V. Cox, L.E. Craig, A.G. Smith and D.G. Smith 1990. *A geological time table*. Cambridge University Press, Cambridge, 265 pp.
- Hassan, T.H. 1989. The Lower and Middle Jurassic in offshore Abu Dhabi: stratigraphy and hydrocarbon occurrence. *Proceedings of the 6th Middle East Oil Show, SPE paper no. 18011*, p. 847-858.
- Hasson, F.P. 1985. New observations on the biostratigraphy of the Saudi Arabian Umm er Radhuma Formation (Paleogene) and its correlation with neighboring regions. *Micropalaeontology*, v. 31, p. 335-364.
- Holden, A. and H.M. Kerr 1997. A subsurface lithostratigraphic subdivision of the Hauterivian to Aptian Furt (informal) and Qishn formations, Yemen. *Marine and Petroleum Geology*, v. 14, p. 631-542.
- Howarth, M.K. and N.J. Morris 1998. The Jurassic and Lower Cretaceous of Wadi Hajar, southern Yemen. *Bulletin of the Natural History Museum, Geology series*, v. 54, p. 1-32.
- Hughes, G.W., O. Varol and Z.R. Beydoun 1991. Evidence for Middle Oligocene rifting of the Gulf of Aden and for Late Oligocene rifting of the southern Red Sea. *Marine and Petroleum Geology*, v. 8, p. 354-358.
- Hughes, G.W. 2000. Bioecostratigraphy of the Shu'aiba Formation, Shaybah field, Saudi Arabia. *GeoArabia*, v. 5, no. 4, p. 545-578.
- Hughes Clark, M.W. 1988. Stratigraphy and rock unit nomenclature in oil producing areas of Interior of Oman. *Journal of Petroleum Geology*, v. 11, p. 5-60.
- Husseini, M.I. 1988. The Arabian Intracambrian extensional system. *Tectonophysics*, v. 148, p. 93-103.
- Johnson, J.G., G. Klapper and C.A. Sandberg 1985. Devonian eustatic fluctuations of Euramerica. *Geological Society of America Bulletin*, v. 96, p. 567-587.
- Keeley, M.L. 1989. The Paleozoic history of the Western Desert of Egypt. *Basin Research*, v. 2, p. 35-48.
- Konert, G., A.M. Al-Afifi and S.A. Al-Hajri 2001. Paleozoic stratigraphy and hydrocarbon habitat of the Arabian Plate. *GeoArabia*, v. 6, no. 3, p. 407-422.
- Le Nindre, Y-M., J. and H. Manivit and D. Vaslet 1990. Stratigraphie séquentielle du Jurassique et du Crétacé en Arabie Saoudite. *Bulletin of the Geological Society of France*, v. 5, p. 1025-1034.
- Lenz, A.C. 1982. Ordovician to Devonian sea-level changes in western and northern Canada. *Canadian Journal of Earth Sciences*, v. 19, p. 1919-1932.
- Loutfi, G. and M.M. Abdel Sattar 1987. Geology and hydrocarbon potential of the Triassic succession in Abu Dhabi, UAE. *Proceedings of the 5th Society of Petroleum Engineers Middle East Oil Conference, Bahrain*. SPE paper no. 15698, p. 717-734.
- Mahmoud, M.D., D. Vaslet and M.I. Husseini 1992. The Lower Silurian Qalibah Formation of Saudi Arabia: an important hydrocarbon source rock. *American Association of Petroleum Geologists Bulletin*, v. 76, p. 1491-1506.

- McGillivray, J.G. and M.I. Hussein 1992. The Paleozoic petroleum geology of central Arabia. *American Association of Petroleum Geologists Bulletin*, v. 76, 1473-1490.
- Miller, K.G., et al. 1996. Drilling and dating New Jersey Oligocene-Miocene sequences: ice volume, global sea level and Exxon records. *Science*, v. 271, p. 1092-1094.
- Mitchum, R.M., Jr. and M.A. Uliana 1988. Seismic stratigraphy of carbonate depositional sequences, Upper Jurassic-Lower Cretaceous, Neuquen Basin, Argentina. *American Association of Petroleum Geologists Bulletin Memoirs*, v. 39, p. 255-274.
- Nolan, S.C., P.W. Skelton, B.P. Clissold and J.D. Smewing 1990. Maastrichtian to Early Tertiary stratigraphy and palaeogeography of the central and northern Oman Mountains. In, A.H.F. Robertson, M.P. Searle and A.C. Ries (Eds.), *The Geology and Tectonics of the Oman Region*. Geological Society, London, Special Publication no. 49, p. 495-519.
- Pascoe, R.P., N. Evans and T. Harland 1995. The generation of unconformities within the Mishrif and Laffan formations of Dubai and adjacent areas. In, M.I. Al-Husseini (Ed.), *Middle East Petroleum Geosciences, GEO'94*. Gulf PetroLink, Bahrain, v. 2, p. 749-760.
- Pekar, S. and K.G. Miller 1996. New Jersey Oligocene 'Icehouse' sequences (ODP Leg 150X) correlated with global $\delta^{18}O$ and Exxon eustatic records. *Geology*, v. 24, no. 6, p. 567-570.
- Philip, J., J. Borgomano and A. Al-Maskiry 1995. Cenomanian-Early Turonian carbonate platform of northern Oman: stratigraphy and palae-environments. *Paleogeography, Paleoclimatology, Paleocology*, v. 119, p. 77-92.
- Plint, A.G., N. Eyles, C.H. Eyles and R.G. Walker 1992. Controls of sea-level changes. In, R.J. Walker and N.P. James (Eds.), *Facies Models: Response to Sea-Level Change*. Geological Association of Canada, St. Johns, Newfoundland, p. 15-25.
- Powers, R.W. 1968. *Lexique stratigraphique international*. Volume III, Asie, Fas. 10 b1, Arabia Saoudite. Centre Nationale de la Recherche Scientifique, Paris, 177 p.
- Qahtani, A.M. et al., 2002. Factors concerning the development, distribution and preservation of reservoir facies in Jurassic carbonates and their impact on petroleum systems in eastern and northern Saudi Arabia. *American Association of Petroleum Geologists, International Petroleum Conference and Exhibition, Cairo, Egypt, Abstracts*, p. 31.
- Röhl, U. and J.G. Ogg 1996. Aptian-Albian sea level history from guyots of western Pacific. *Paleoceanography*, v. 11, p. 595-624.
- Ross, C.A. and J.P. Ross 1988. Late Paleozoic transgressive-regressive deposition. *Society of Economic Paleontologists and Mineralogists, Special Publication*, v. 42, p. 227-247.
- Stoll, H. and D.P. Schrag 2000. High-resolution stable isotope record from Upper Cretaceous rocks of Italy and Spain: glacial episodes in a greenhouse planet? *Geological Society of America Bulletin*, v. 112, p. 308-319.
- Schandelmeier, H. and P.O. Reynolds 1997. *Palaeogeographic-palaeotectonic atlas of the north-eastern Africa, Arabia and adjacent areas*. Balkema, Rotterdam, The Netherlands, 160 p.
- Senalp, M. and A.A. Al-Duaiji 1995. Stratigraphy and sedimentation of the 'Unayzah and Khuff reservoir, central Arabia'. In, M.I. Al-Husseini (Ed.), *Middle East Petroleum Geosciences, GEO'92*. Gulf PetroLink, Bahrain, v. 2, p. 837-847.
- Senalp, M. and A.A. Al-Duaiji 2001a. Sequence stratigraphy of the 'Unayzah and reservoir, central Saudi Arabia. *Saudi Aramco Journal of Technology*, Summer 2001, p. 20-43.
- Senalp, M. and A.A. Al-Duaiji 2001b. Qasim Formation: Ordovician storm- and tide-dominated shallow-marine siliciclastic sequences, Central Saudi Arabia. *GeoArabia*. v. 6, no. 2, p. 233-268.
- Sharland, P.R., R. Archer, D.M. Casey, R.B. Davies, S.H. Hall, A.P. Heward, A.D. Horbury and M.D. Simmons 2001. *Arabian Plate Sequence Stratigraphy*. *GeoArabia, Special Publication 2, Bahrain*. 371 pp. and 3 enclosures.
- Sharland, P.R., D.M. Casey, R.B. Davies, M.D. Simmons and O.E. Sutcliffe 2004. *Arabian Plate sequence stratigraphy*. *GeoArabia*, v. 9, no. 1, p. 199-214 and 2 posters.
- Simmons, M.D. 1990. Aspects of the micropalaeontology and stratigraphy of Cretaceous shelf carbonates from the Oman Mountains. Unpublished PhD thesis, Council for National Academic Awards, UK.
- Smith, A.B., N.J. Morris and A.S. Gale 1995. Late Cretaceous carbonate platform faunas of the United Arab Emirates-Oman border region. *Bulletin of the Natural History Museum, London*, v. 51, p. 91-119.
- Stoll, H.M. and D.P. Schrag 2000. High-resolution stable isotope records from Upper Cretaceous rocks of Italy and Spain: glacial episodes in a greenhouse planet? *Geological Society of America Bulletin*, v. 112, p. 308-319.
- Sugden, W. and A.J. Standring 1975. Qatar Peninsula. In, *Lexique Stratigraphique International*, v. III Asie, Centre National de la Recherche Scientifique, Paris, fasc. 10b3., 120 p.
- Vail, P.R., R.M. Mitchum Jr. and S. Thompson III 1977. Seismic stratigraphy and global changes in sea level. Part 4: Global cycles of relative changes of sea level. *American Association of Petroleum Geologists Memoirs*, v. 26, p. 83-97.

- Vaslet, D. 1990. Upper Ordovician glacial deposits in Saudi Arabia. *Episodes*, v. 13, p. 147-161.
- Weijermars, R. 1999. Surface geology, lithostratigraphy and Tertiary growth of the Dammam Dome, Saudi Arabia: a new field guide. *GeoArabia*, v. 4, no. 2, p. 199-226.
- Wender, L.E., J.W. Bryant, M.F. Dickens, A.S. Neville and A.M. Al-Moqbel 1998. Paleozoic (pre-Khuff) hydrocarbon geology of the Ghawar area, eastern Saudi Arabia. *GeoArabia*, v. 3, no. 2, p. 273-302.
- Wilson, A.O. 1985. Depositional and diagenetic facies in the Jurassic Arab-C And -D reservoirs, Qatif field, Saudi Arabia. In, P.O. Roehl and P.W. Choquette (Eds.), *Carbonate Petroleum Reservoirs: A Casebook*. Springer-Verlag, New York, p. 319-340.
- Yahi, N., R.G. Schaefer and R. Littke 2001. Petroleum generation and accumulation in the Berkine basin, eastern Algeria. *American Association of Petroleum Geologists Bulletin*, v. 85, no. 8, p. 1439-1467.
- Yousif, S. and G. Nouman 1997. Jurassic geology of Kuwait. *GeoArabia*, v. 2, no. 1, p. 91-110.
- Ziegler, M.A. 2001. Late Permian to Holocene paleofacies evolution of the Arabian Plate and its hydrocarbon occurrences. *GeoArabia*, v. 6, no. 3, p. 445-504.

ABOUT THE AUTHORS

Bilal U. Haq received his PhD and DSc in Geology from the University of Stockholm, Sweden. He has conducted research at the Woods Hole Oceanographic Institution, Exxon Production Research Labs in Houston and the National Science Foundation in Washington, DC and has held assignments with the White House and the World Bank. Bilal's research has included paleoceanography, paleobiogeography, paleoclimatology, sequence stratigraphy and global sea-level change, natural gas hydrates, and global warming and its impact on maritime economies. He has participated in four ocean drilling expeditions to the Pacific, Indian and Southern Oceans, in the last two as the co-chief Scientist. He has published extensively on many topics in marine geosciences and authored or co-authored over 150 papers and books. Bilal's papers on paleoceanography, sequence stratigraphy and sea level changes of the past have been among some of the most cited publications in *Sedimentary Geology* for more than a decade. He has been an American Association of Petroleum Geologists' Distinguished Lecturer and was awarded the Francis P. Shepard Medal for excellence in Marine Geology by the Society for Sedimentary Geology (Society for Economic Paleontologists and Mineralogists). He was conferred honorary professorships by Tongji University in Shanghai and by the Academia Sinica Institute of Oceanology in Qingdao, China. Bilal was elected a Fellow by the Geological Society of America and by the American Association for the Advancement of Science. He also received the National Science Foundation's Antarctic Medal and was recently awarded the Ocean Sciences Award by the American Geophysical Union for "significant contributions and services to ocean sciences".



bhaq@netscape.com

Abdul Motaleb Al-Qahtani holds a BSc in Geology from King Saud University (1983), Riyadh, and MSc in Geophysical Engineering from Colorado School of Mines (1988). He has over two decades of exploration experience in subsurface geological/geophysical mapping and evaluating hydrocarbon plays and prospects. Abdul Motaleb has written about and presented several exploration topics concerning Paleozoic and Mesozoic stratigraphy of the Arabian Platform and subsurface mapping in the Gulf region and at AAPG. He held various assignments in geophysical technology, processing, acquisition and petroleum exploration/seismic interpretation (Chevron) prior to joining Regional Mapping and Special Studies of Area Exploration Department at Saudi Aramco and has since held several technical leadership assignments within the organization. He is presently leading a group to evaluate hydrocarbon plays and prospects in the offshore Arabian Gulf. Abdul Motaleb has also represented Aramco on the Stratigraphic Committee of the Arabian Gulf in the Gulf Cooperation Council (GCC). He is a member of the AAPG, SPE and Dhahran Geosciences Society.



abdelmottaleb.qahtani@aramco.com

Manuscript received March 31, 2003

Revised October 12, 2004

Accepted November 21, 2004

Press version proofread by Authors February 22, 2005